Radiology

Improving Safety of MRI in Patients with Deep Brain Stimulation Devices

Alexandre Boutet, MD • Clement T. Chow, BKin • Keshav Narang, BMSc • Gavin J. B. Elias, BA • Clemens Neudorfer, MD • Jürgen Germann, MSc • Manish Ranjan, MBBS • Aaron Loh, MB, BCh, BAO • Alastair J. Martin, PhD • Walter Kucharczyk, MD • Christopher J. Steele, PhD • Ileana Hancu, PhD • Ali R. Rezai, MD • Andres M. Lozano, MD

From the University Health Network, Toronto, Canada (A.B., C.T.C., K.N., G.J.B.E., C.N., J.G., A.L., W.K., A.M.L.); Joint Department of Medical Imaging, University of Toronto, Toronto, Canada (A.B., W.K.); Department of Neurosurgery, West Virginia University, Morgantown, WVa (M.R., A.R.R.); Department of Neurosurgery, Rockefeller Neuroscience Institute, Morgantown, WVa (M.R., A.R.R.); Department of Radiology and Biomedical Imaging, University of California, San Francisco, San Francisco, Calif (A.J.M.); Department of Psychology, Concordia University, Montreal, Canada (C.J.S.); Department of Neurology, Max Planck Institute for Human Cognitive and Brain Sciences, Leipzig, Germany (C.J.S.); Center for Scientific Review, National Institutes of Health, Bethesda, Md (I.H.); and Division of Neurosurgery, Department of Surgery, Toronto Western Hospital and University of Toronto, 399 Bathurst St, WW 4-437, Toronto, ON, Canada M5T 2S8 (A.M.L.). Received October 11, 2019; revision requested November 20; final revision received February 13, 2020; accepted February 20. **Address correspondence to** A.M.L. (e-mail: *lozano@uhnresearch.ca*).

Supported by the RR Tasker Chair in Functional Neurosurgery at University Health Network. K.N. supported by the Jane & Howard O. Jones Bursary Fund. C.N. supported by the German Research Foundation (Deutsche Forschungsgemeinschaft, DFG NE 2276/1-1). The opinions expressed in this article are the authors' own and do not reflect the views of the National Institutes of Health, the Department of Health and Human Services, or the United States government.

Conflicts of interest are listed at the end of this article.

Radiology 2020; 296:250–262 • https://doi.org/10.1148/radiol.2020192291 • Content codes: NR MR

MRI is a valuable clinical and research tool for patients undergoing deep brain stimulation (DBS). However, risks associated with imaging DBS devices have led to stringent regulations, limiting the clinical and research utility of MRI in these patients. The main risks in patients with DBS devices undergoing MRI are heating at the electrode tips, induced currents, implantable pulse generator dysfunction, and mechanical forces. Phantom model studies indicate that electrode tip heating remains the most serious risk for modern DBS devices. The absence of adverse events in patients imaged under DBS vendor guidelines for MRI demonstrates the general safety of MRI for patients with DBS devices. Moreover, recent work indicates that—given adequate safety data—patients may be imaged outside these guidelines. At present, investigators are primarily focused on improving DBS device and MRI safety through the development of tools, including safety simulation models. Existing guidelines provide a standardized framework for performing safe MRI in patients with DBS devices. It also highlights the possibility of expanding MRI as a tool for research and clinical care in these patients going forward.

Online supplemental material is available for this article.

Online SA-CME • *See www.rsna.org/learning-center-ry*

Learning Objectives:

After reading the article and taking the test, the reader will be able to:

- Identify the main risks of performing MRI for deep brain stimulation (DBS) devices
- List the common dosimetric indexes used to define specific heating-related thresholds for DBS devices and discuss their limitations
- Identify techniques and tools to improve MRI safety for patients with DBS devices

Accreditation and Designation Statement

The RSNA is accredited by the Accreditation Council for Continuing Medical Education (ACCME) to provide continuing medical education for physicians. The RSNA designates this journal-based SA-CME activity for a maximum of 1.0 *AMA PRA Category 1 Credit*™. Physicians should claim only the credit commensurate with the extent of their participation in the activity.

Disclosure Statement

The ACCME requires that the RSNA, as an accredited provider of CME, obtain signed disclosure statements from the authors, editors, and reviewers for this activity. For this journal-based CME activity, author disclosures are listed at the end of this article.

Deep brain stimulation (DBS) modulates aberrant neural circuits implicated in a broad range of neurologic disorders (1). Most commonly used in movement disorders such as Parkinson disease, dystonia, and tremor, DBS is also investigated for use in psychiatric and cognitive disorders such as depression and Alzheimer disease (2). Estimates show 150 000 patients have undergone surgical procedures for DBS worldwide (3). Approximately 70% of these patients will require an MRI within 10 years of implantation (4). However, past adverse MRI-related incidents led to strict guidelines restricting access to imaging for patients with DBS devices (5). In addition to constraining the diagnostic utility of MRI in this population, these regulations substantially impede MRI-based research.

The DBS literature reports five cases of injury involving radiofrequency (RF) currents—three MRI-related (Table 1), which prompted a 2005 U.S. Food and Drug Administration warning regarding patients with DBS devices undergoing MRI (6). To prevent additional injuries, DBS hardware vendors (ie, Medtronic, Boston Scientific, and Abbott) established MRI guidelines for imaging patients with DBS devices (5,7). These vendors approved and produced MRI-conditional DBS devices. Vendor guidelines restrict MRI coil types and gradient settings, as well as scan only at specific magnetic field strengths (ie, 1.5 T)

Abbreviations

B_{1+RMS} = root-mean-square value of the MRI effective component of the RF magnetic (B_1) field, DBS = deep brain stimulation, IPG = implantable pulse generator, RF = radiofrequency, SAR = specific absorption rate

Summary

Performance of MRI with deep brain stimulation devices carries risks, but developed tools aim to improve safety and expand the role of MRI in clinical care and research for these patients.

Essentials

- The most studied risks of performing MRI with deep brain stimulation (DBS) devices include device heating, induced currents, implantable pulse generator dysfunction, and magnetic field–induced device movement.
- Device heating and resultant neuronal damage remains the most serious risk for performing MRI with modern DBS devices.
- MRI performed under DBS vendor guidelines for MRI report no adverse events.
- Following local safety testing to characterize the risks, acquiring optimal functional neuroimaging data safely outside prescribed DBS vendor guidelines for MRI could provide insight into pathologic brain states, as well as the structural and functional changes associated with active DBS therapy.
- At present, tools to improve DBS safety including safety simulation models aimed to expand clinical and research use of MRI in these patients.

and specific heating-related thresholds (eg, specific absorption rate [SAR] ≤0.1 W/kg and root-mean-square value of the MRI effective component of the RF magnetic [B_1] field [B_{1+RMS}] <2 μT) (8,9). These guidelines mainly aim to prevent MRI-induced device heating, which could lead to substantial brain damage (6). Recently, some constraints limiting brain MRI of patients with DBS devices have been relaxed, with certain newer DBS device models deemed full-body eligible (8–10).

Since the first reported use of MRI in patients with DBS devices, phantom models have been the most common tool to improve our understanding of DBS device and MRI safety (Fig 1). Phantom models allow investigators to simulate, albeit with limitations, how DBS devices behave during MRI scanning under safe and controlled conditions (5). However, a growing number of investigators now embrace newer techniques such as computer simulation to improve safety.

Enhanced knowledge of MRI safety in patients with DBS devices could lead to more proportionate safety guidelines, thereby improving patient care. Tagliati et al (11) found that nearly half the centers they surveyed were not performing brain MRI in patients with DBS devices. Moreover, only 13% of centers reported performing MRI of other body parts. These numbers are particularly worrisome given that MRI has become the reference standard for imaging many neurologic pathologic conditions (including surgical emergencies such as suspected spinal cord or cauda equina compression), as well as a range of musculoskeletal and abdominal pathologic conditions. In fact, 66%–75% of patients diagnosed with Parkinson disease, essential tremor, or dystonia will need an MRI in the 10 years following an operation for DBS (4). Most of these MRI examinations (62%) would be body MRI unrelated to the primary neurologic or neuropsychiatric diagnosis. Furthermore, higher field strength (eg, 3.0 T and 7.0 T) and less common sequences (eg, functional MRI and diffusion-weighted imaging) continue to show potential for clinical and research use. Investigation of medical implant safety under these conditions generates considerable interest (12–15). For example, functional MRI allows visualization of brain activity changes as a result of stimulation, revealing clinically efficacious networks in Parkinson disease (16,17) and obsessive-compulsive disorder (18). Also, functional MRI demonstrates the motor and nonmotor cortical segregation of the subthalamic nucleus, which is a structure targeted for Parkinson disease (19). Similarly, diffusion-weighted imaging commonly assesses stroke, assists neurosurgical planning, and provides disease markers (20,21). However, DBS vendor guidelines remain highly restrictive and often prohibit using both routine clinical (eg, DBS electrode localization [22]) and research (eg, arterial spin-labeling [12]) protocols (23,24).

MRI-related Risks of DBS Devices

Standards related to MRI safety testing of neurostimulators are based on the American Society for Testing and Materials International (25–27), International Organization for Standardization Technical Standard or ISO/TS 10974 (28), and other documents (29). A detailed description of these constantly evolving standards is beyond the scope of this review. Below is a summarization of the most common MRI risks studied in the literature (26). However, other potential risks remain, such as gradient field–induced vibrations.

Heating

Heating of DBS devices and the potential for subsequent brain damage constitutes the main risk when performing MRI in patients with neurostimulators (30–32). RF pulses applied during MRI elicit a detectable signal in bodily tissue and thereby acquire images of the target structures. These pulses may induce high currents in DBS electrodes and extension wires (5,33,34). Specifically, provided a conductive system (the extension wire and lead in the case of DBS) of appropriate length, the rapidly changing magnetic fields during RF excitation induce a current (ie, the antenna effect) (35). Then, the induced current dissipates as heat at the electrode tip. This is the location where the electrical current flux density is highest (and with highest resistance) (36). Because permanent brain damage can occur at temperatures exceeding 45°C (113°F) (ie, 7°C–8°C [45°C–46°F] in excess of normal body temperature) (37), temperature increases of less than 2°C (36°F) are felt to be acceptable and within a sufficient margin of safety (12,38–40). In addition to improving patient safety, minimizing MRI-induced heating could also improve data quality. For example, because blood oxygen level–dependent signal may be altered by a change in temperature, the minimization of DBS device heating may improve functional MRI data quality (39,41).

Table 1: Injuries in Patients with DBS Devices

Study	DBS Placement	IPG	Modality	Outcome	Case Description
Nutt et al, 2001 (106); Ruggera et al, 2003 (107)	Bilateral STN	Bilateral (placement not specified)	Diathermy	Death	Use of diathermy during a dental procedure caused peri-electrode edema and neurologic changes (decerebrate posturing; occasional myoclonic jerks; small, questionably reactive pupils; weak corneal responses; and bilateral Babinski signs) and eventually death
U.S. FDA report, 2001 (108)	Bilateral GPi and STN	Not specified	Diathermy	Permanent	Use of spinal diathermy caused peri-electrode edema (and possible hemorrhage) and permanent neurologic changes (aphasic with right hemiplegia, eye deviation to the left, and a Babinski sign)
Spiegel et al, 2003 (109)	Bilateral STN	Externalized	1.0-T brain MRI (four SE sequences; TR, 570 msec; TE, 15 msec)	Temporary	Temporary neurologic changes (continuous dystonic extensions of the left foot and sudden ballistic movements of the left leg with abduction) with full recovery in the following weeks. No acute findings at head CT
Henderson et al, 2005 (110)	Bilateral STN	Bilateral (subclavicular and abdominal)	1.0-T spine MRI (no sequence details provided)	Permanent	Peri-electrode edema and hemorrhage and permanent neurologic changes (dysarthria, right hemiparesis, and dysconjugate gaze)
Zrinzo et al, 2011 (111)	Not specified	Externalized	1.5-T brain MRI (T2-weighted FSE; TR, 3000 msec; TE, 95 msec)	Temporary	Temporary neurologic changes (dyskinetic agitation and head movements). No acute findings on MRI localizer

Note.—Short-wave diathermy uses radiofrequency and it has been used to accelerate tissue healing by using local heating in several muscular conditions. DBS = deep brain stimulation, FDA = Food and Drug Administration, FSE = fast spin echo, GPi = globus pallidus internus, IPG = implantable pulse generator, SE = spin echo, STN = subthalamic nucleus, TE = echo time, TR = repetition time.

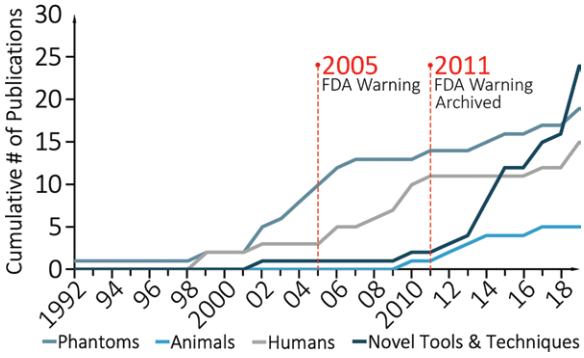

Figure 1: Graph shows safety studies over time (cumulative number of deep brain stimulation–related MRI safety studies published from 1992 to 2019). These studies were categorized into phantom, animal, and human safety studies, as well as tools and techniques. Note recent sharp increase in number of studies focusing on innovative tools and techniques. FDA = Food and Drug Administration.

DBS device heating is related to both intrinsic and extrinsic factors (Fig 2). Extrinsic factors include the amount of RF energy applied, related to the SAR and B_{1+RMS} (5). These metrics are used to estimate implant heating (42). The magnetic field strength and the type of MRI coils also constitute extrinsic factors. When using body-transmit coils, a larger proportion of the DBS device hardware is exposed to the RF pulses compared with head-transmit coils; as such, body-transmit coils cause more device heating (12,33,39,43). Intrinsic factors, such as the type of neurostimulator, may also influence temperature rise. Different brands and models of DBS device components (ie, electrodes, extension wire, and implantable pulse generator [IPG]) may exhibit different temperature increases based on their electrical characteristics (32). The geometry of the implanted device within the patient can also contribute to heating (12,33). The configuration of the implant is often institution-specific and varies in terms of electrode quantity, placement of excess extension wires, and IPG positioning. Finally, patients' position in reference to the MRI bore and coils may further influence heating (39).

Measures of Heating

MRI guidelines specify heating-related thresholds (ie, SAR and B_{1+RMS}) to prevent brain injury. Historically, SAR, a dosimetric index characterizing the thermogenic aspects of an electromagnetic field, commonly estimates energy deposition during MRI (7). However, SAR has inherent limitations, namely that its calculations vary by MRI system manufacturer and is derived by using various evolving assumptions and models of the human body by manufacturers (7,44,45). These limitations might explain why B_{1+RMS}—a measure of the average magnetic field generated by the RF transmit coil—may provide an alternative dosimetric index to SAR (42). Unlike SAR, B_{1+RMS} is independent of the patient's weight, vendor-specific assumptions, and MRI hardware and software. It is a requirement of the International

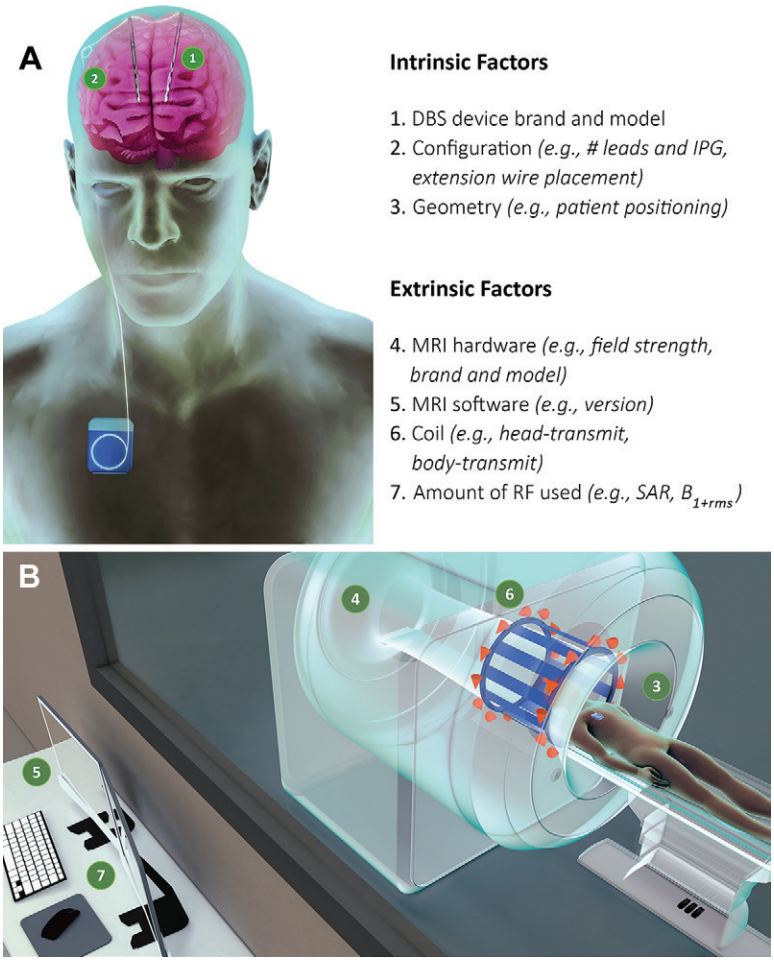

Figure 2: Images show risk factors for deep brain stimulation (DBS) device heating. Summary of main risk factors contributing to DBS device heating are shown on, *A*, three-dimensional model of patient with DBS and, *B*, on three-dimensional model of MRI suite. Risk factors intrinsic and extrinsic to DBS device are labeled and listed. B_{1+RMS} = root-mean-square value of MRI effective component of RF magnetic (B_1) field, IPG = implantable pulse generator, RF = radiofrequency, SAR = specific absorption rate.

Electrotechnical Commission that newer MRI software provide this measure (29). However, B_{1+RMS} lacks peer-reviewed evidence to confirm its role as a viable alternative (45). Although SAR and B_{1+RMS} are useful for establishing precautionary measures regarding global tissue heating in patients, they are less informative when DBS implants are present. SAR and B_{1+RMS} measure the energy deposited globally in the patient and not specifically at the implant, as they assume heating is uniform within the field of view (46–48). Crucially, both indexes fail to account for the localized high-RF electric fields (and potentially heating) at the electrode tips and thus should be interpreted cautiously.

To prevent dangerously high levels of DBS device heating, dosimetric indexes (ie, global SAR and B_{1+RMS}) restrict the MRI acquisition parameters. To follow the recommended MRI guidelines, routinely used clinical MRI protocols may need modification to decrease their SAR and/or B_{1+RMS}. This can involve reducing the number of slices, flip angles, and number of echoes, or increasing the repetition time (49). Such modifications typically necessitate the presence of those with a specialized knowledge base (ie, radiologists and physicists) and may result in compromised image quality (ie, signal-to-noise ratio and contrast-to-noise ratio) and/or increased acquisition time (49,50). Moreover, reducing the number of slices requires radiologists' supervision to ensure the area in question remains in the field of view. Pulse sequences with larger and more frequent RF pulses have higher SAR and B_{1+RMS}. Spin-echo images using large pulses (eg, fluid-attenuated inversion recovery) and fast spin-echo images using rapid pulses (eg, T2-weighted sequences) deliver more RF power, increasing their likelihood of causing heating. Conversely, gradient-echo images (eg, gradient-recalled echo–echo-planar imaging) use smaller and more frequent RF pulses, generally considered safer for patients with DBS implants (49). In sum, with specialized knowledge and clinical expertise, MRI usage in patients with DBS may be slightly expanded with modifications of routine clinical MRI protocols to remain within approved limits of SAR and/or B_{1+RMS}.

Induced Currents

MRI can induce currents in DBS hardware through two processes. First, RF pulses and gradient switchings cause time-varying magnetic fields capable of inducing impulses in the circuit, consisting of the pulse generator, leads, electrodes, and brain matter (35). Second, the antenna effect is also responsible for induced currents in addition to heating (35,36). Because RF currents have a carrier frequency in the megahertz range, they would not normally induce neuronal activity (ie, action potentials) (39,51). Gradient switching, however, may induce currents at lower frequencies (low kilohertz range) associated with neuronal firing (39). Depending on the position of the electrodes relative to neuroanatomic structures and fiber bundles, these currents could cause patient discomfort (eg, paresthesias, muscle spasms) or potentially more severe adverse effects such as seizures (52). Unintended stimulation and tissue damage produced by gradient-induced lead voltage, as well as tissue damage due to rectification produced by RF-induced lead voltage, should be monitored as per the standards (25,27,28).

IPG Dysfunction

Magnetic fields produced by MRI hardware could interfere with IPG function (27). Older IPG models (eg, Itrel II; Medtronic, Minneapolis, Minn) relied on a magnetic reed switch to turn the device on or off. Depending on the patients' position relative to the MRI magnetic field, these reed switches could theoretically become spontaneously activated during MRI scanning, with the potential to harm patients and damage DBS components or alter settings (53). Whereas the most commonly used newer IPG models may not have magnetic reed switches, device malfunction induced by static magnetic fields, gradients, or RF fields should nonetheless be tested for following imaging as per the standards (25,27,28).

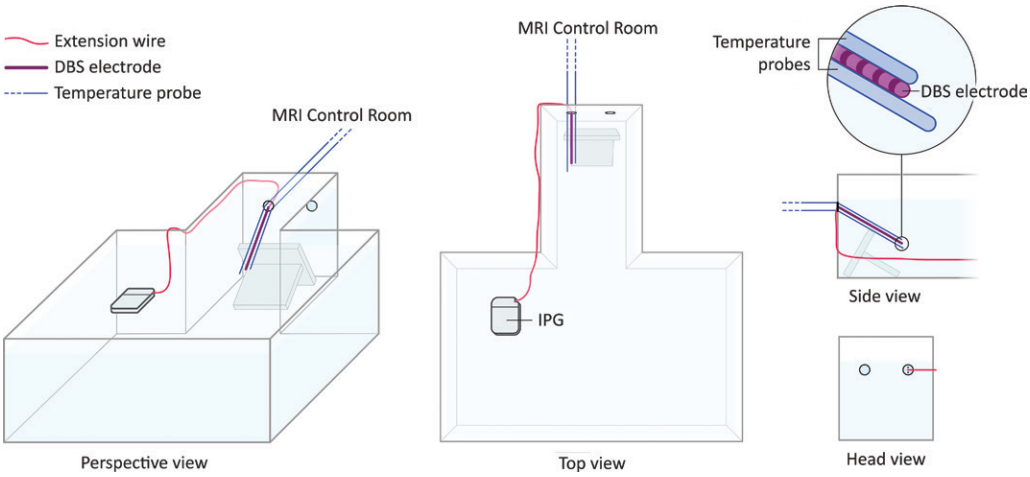

Figure 3: Image shows schematic representations of Lucite phantom model used during experiments. Experiment 1 configuration is represented. DBS = deep brain stimulation, IPG = implantable pulse generator. (Reprinted, with permission, from reference 12.)

Magnetic Field–induced Device Movement

As modern components of MRI-conditional neurostimulators are nonmagnetic or diamagnetic, strong mechanical forces are not expected (5). Older IPG models (ie, Itrel; Medtronic) contained residual magnetic materials, such as sealing chips, ferrite core antennae, and reed switches (53,54). The magnetic component in newer IPG models should be minimal because leads and extension wires are nonmagnetic (55–57). Because the magnetic force in the MRI isocenter is theoretically minimal (owing to the high homogeneity of the magnetic field), one would expect the mildly magnetic IPG components located at the periphery to be most sensitive to mechanical forces (54).

Phantom Safety Studies

Since 1992, more than 15 studies described the use of phantom models to investigate the safety of DBS during MRI (Table E1 [online]). Device heating and, to a lesser extent, IPG function and device movement were most commonly assessed. Except for one study that examined thoracic area MRI (34), phantom studies have only assessed brain MRI safety. As such, the following section concerns brain MRI.

Per the American Society for Testing and Materials F2182 and ISO/TS 10974 standards (25,28), phantoms, defined as standardized containers filled with a medium that simulates the electrical and thermal properties of the human body (Fig 3), should measure RF-induced heating near the DBS device during MRI. These standards are subject to improvement for better estimate of heating (58). The most commonly used medium in phantom studies has been semisolid gel containing polyacrylic acid. The gelling agent prevents the transportation of phantom material that is locally heated by thermal convection (59). In addition, it simulates the permittivity and conductivity of various tissues in the frequency range of interest (60). The temperature should be recorded at the location suspected to have the highest amount of heating. In the case of a DBS device, this is the most distal uninsulated contact of the stimulating electrode. If substantial heating is detected, then computational modeling may refine the safety testing by simulating conditions in vivo. However, phantom models are limited by their lack of perfusion—thereby failing to replicate heat dissipation and the thermoregulatory effects of blood flow—and their inability to reproduce the thermodynamics of the human brain (6). Nonetheless, these experiments provide invaluable opportunities to explore implant safety outside of DBS vendor guidelines for MRI.

Although DBS devices have evolved, they continue to be implanted in similar configurations (ie, linear conductive wire), meaning that heating due to the antenna effect remains a major concern. Unacceptable temperature rises (ie, >2°C [36°F]) at the electrode tips have been reported in phantom models with pulse sequences using excessive SAR (37,61), with higher magnetic field strength (12,51), and with different DBS device configurations (62). Because of the constantly evolving nature of MRI hardware, DBS devices, and surgical techniques, the data from these studies may not be readily applicable to today's conditions.

Extrinsic factors related to DBS device heating vary across phantom studies. First, as expected, higher field strengths are generally associated with greater temperature rises. However, the difference in temperature rises between 3.0 T and 1.5 T was less than 1°C (34°F) in recent studies (16,39). Interestingly, variations in MRI hardware and software systems contribute to inconsistencies in temperature rises. Notably, Baker et al (7,44) demonstrated that two different-generation MRI systems from the same manufacturer, using similar coils and RF-deposited energy, nonetheless triggered different temperature changes; they concluded that console-reported SAR in patients with DBS devices is an unreliable predictor of heating. Second, studies examined the relationship between coil type (ie, head-transmit or body-transmit coil) and temperature rise. Strikingly, Rezai et al (33) reported a temperature rise as high as 25.3°C (77.5°F) with a body-transmit coil, compared with a rise of 7.1°C (44.8°F) with a head-transmit coil. These results were not reproduced in several recent studies, which showed a difference of less than 1°C (34°F) between both coils (12,16,39,40). The discrepancy might be explained by the fact that Rezai et al (33) studied sequences that used more RF energy than would be used with clinical sequences. This study design modeled extreme scenarios, whereas the more recent reports investigated clinically applicable sequences. Differences in DBS device models may also contribute to these inconsistencies. Finally, phantom models show considerable variation across studies in terms of shape and filling medium. Specifically, the concentration of polyacrylic acid used to make the semisolid flesh-simulating gel reportedly influences

device heating (59). To avoid underestimating device heating, investigators used increasingly higher concentrations of polyacrylic acid over the years.

Phantom model studies had inconsistencies in intrinsic factors related to DBS device heating. First, many experiments date back to the early 1990s, testing obsolete DBS models no longer routinely used in clinical practice (33,37,38,44,51,53,59,61–65). Moreover, all but one study (53) exclusively examined Medtronic DBS devices (Table E1 [online]). This limits the applicability of this data to other brands and more recent models because electrical conductivity (and thus heating) properties may vary across DBS devices (5). Second, DBS device configurations may vary in terms of electrode number and IPG, as well as the placement of excess extension wires. Many studies highlight the crucial role of configuration and geometry of devices and their position in the RF electrical fields relative to the coil. For example, phantom model studies commonly report a slightly higher rise in temperature at the left electrode when compared with the right. This might reflect the different position of the left extension wire, which typically connects a left-sided electrode to a right-sided IPG (12,33,51,62). Coiling the excess extension wire exclusively behind the IPG had marked temperature rises as high as 25.3°C (77.5°F); by contrast, partially coiling it at the cranium had maximal rises of only 6.1°C (43°F) (33). Small concentric loops placed on the cranium reduced DBS device heating (66). Nazzaro et al (62) showed that a DBS device configuration with bilateral IPG had higher temperature rise at the electrodes. Finally, short-circuit or open-circuit malfunction created by compromised DBS device integrity (eg, extension breakage) causes sparking (35). DBS vendor guidelines require confirming "normal" DBS device impedances (ie, bipolar current >250 Ω or monopolar current <2000 Ω) (9). Safety data from one group may not apply to different MRI hardware or institutions. Therefore, perform safety testing with MRI hardware and typical DBS configurations on an institution and hardware-specific basis.

Although the use of heating-related thresholds such as SAR and B_{1+RMS} are general predictors of heating, it is unclear to what degree these metrics apply when implants are present. Phantom model studies report a linear relationship between SAR and temperature rise, irrespective of the DBS device and MRI hardware used (7,44). Pulse sequences with higher SAR, such as T2-weighted sequences, tended to cause relatively higher rises in temperature in most studies (12,16,37,38,51). These data suggest a degree of consistency within highly specific environments but confounded by a high degree of variability in induced heat per unit of SAR (Δtemperature rise/SAR) across MRI scanners and software (7,44), and DBS configurations (single compared with bilateral IPG) (62). Therefore, SAR alone cannot estimate absolute temperature rise for different DBS devices and MRI hardware (32). Taking the limitation of measuring implant heating into consideration, SAR less than 1 W/kg during brain MRI has acceptable temperature rises of less than 2°C (36°F) (12,38–40,51,65). Although seldom reported (12,16), a whole-body measure such as B_{1+RMS} likely has similar limitations as SAR. Although supposedly less restrictive (8,9), the presumed advantages of B_{1+RMS} over SAR must be confirmed by additional safety studies.

MRI-induced currents in DBS devices could present additional risks for patients. Phantom studies that investigated IPG output during 1.5-T (39,51,53) or 3.0-T (12) MRI found that gradient switchings can induce up to 1.5 V (39). This value is low when one considers that patients with Parkinson disease or psychiatric disorders commonly receive 3–5 V or 5–7 V, respectively, from their DBS devices (16,67). Low voltages induced by gradient switchings would be unlikely to cause patient discomfort, even when (rarely) superimposed on the IPG pulses. Nevertheless, this mild induced voltage and potential neuronal activity could reduce the sensitivity of an experiment (eg, by using functional MRI to compare "on" vs "off" DBS states). The larger currents induced by RF excitation pulses (up to 7.0 V) (35) should not trigger neuronal activity because their frequency is in the megahertz range (35,39,51).

Prior Medtronic IPG models most commonly reported spontaneous switching between "on" and "off" states and mild movements of the IPG (35,53,65). However, recent studies using Activa models (Medtronic) demonstrated stable IPG output with no indication that gross translational or torque force on the IPG occurred (12,16,39). This finding is important for experiments (eg, using functional MRI) that assume the MRI environment does not disrupt IPG output.

Recent phantom model studies using modern DBS devices and MRI hardware led to safe image acquisition in patients with DBS at 3.0-T MRI by using body-transmit coils (12,16,40). Higher field strengths (>1.5 T) combined with a body-transmit coil crucially provide optimal signal-to-noise ratio and minimize image distortion (39). Phantom models also showed that sequences with research applications, such as functional MRI (12,16,35,40,51,62,64) and diffusion-weighted imaging (12), could be used in patients with DBS in specific conditions. However, arterial-spin labeling, which can measure cerebral blood flow, could not be safely acquired in a recent phantom study (12).

Given that DBS devices continue to use similar configurations (ie, linear conductive wire), heating and, to a lesser extent, induced currents remain the major risks. Generally, lower field strength (ie, 1.5 T) and transmit-receive head coils trigger less DBS device heating than do 3.0-T and body-transmit coils. However, recent phantom studies show that this increased heating is much smaller than suggested by older studies. Heating also varies unpredictably across MRI scanners, software, and DBS device configurations. Conversely, mechanical forces and IPG dysfunction appear to be less of a concern with modern DBS device models due to advances in hardware technology. These findings are limited to modern Medtronic devices. Finally, data from most phantom studies do not readily apply to today's conditions due to constantly evolving MRI hardware, DBS devices, and surgical techniques.

Animal and Human Studies

DBS safety studies in animals provide the opportunity to perform postmortem examinations following MRI scanning to assess for peri-electrode brain damage. Human safety data are also crucial, providing the necessary clinical translation piece after adequate safety data has been gathered by using other methods.

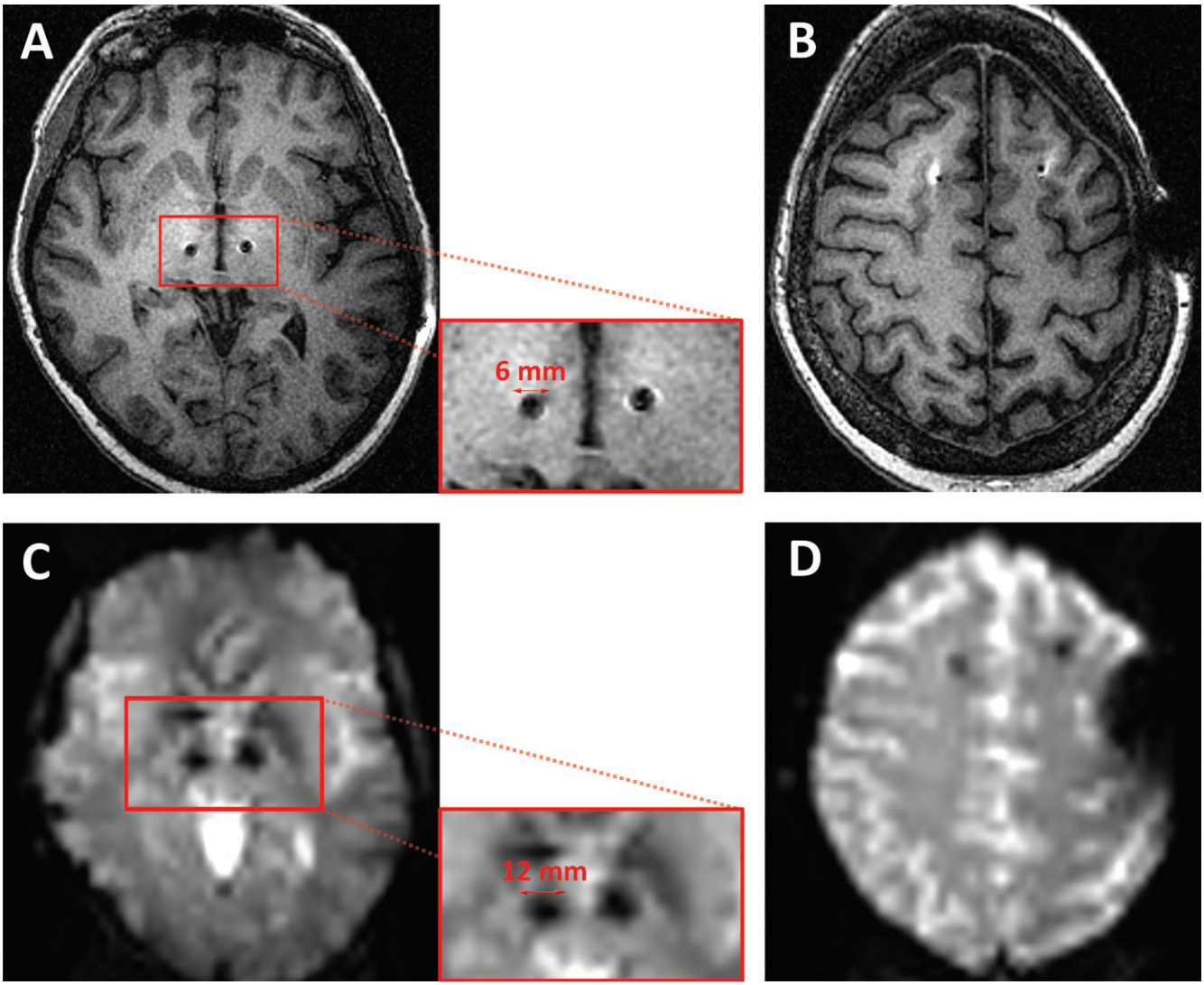

Figure 4: Images show example of three-dimensional (3D) spoiled gradient-recalled acquisition in steady state (SPGR) and gradient-recalled echo (GRE)–echo-planar imaging in patient with deep brain stimulation (DBS) device. *A, B,* Select axial 3D SPGR and, *C, D,* GRE echo-planar images acquired with 3.0-T MRI in a patient with Parkinson disease with DBS electrodes located bilaterally in subthalamic nucleus. Artifact along distal DBS lead measures 6 mm and 12 mm for, *A,* 3D SPGR and, *C,* GRE echo-planar imaging, respectively. Images with red frame are zoomed-in views of *A* and *C.* Subgaleal coiled DBS extension wire creates left parietofrontal artifact in *B* and *D.* (Reprinted, with permission, from reference 12.)

The animal model safety literature has many major limitations. Most notably, no studies have simultaneously investigated both temperature rise and histopathologic changes in perielectrode brain tissue (Table E2 [online]). Nevertheless, this body of work again demonstrates the importance of DBS device geometry relative to the RF coil. Unconventional device positions, such that DBS leads lie perpendicular to the MRI magnetic field (68) or that the cranial extension loop is placed laterally on the head (69), triggered markedly higher temperature increases. These results highlight the importance of standardized device implantation and patient positioning during MRI.

Human safety studies provide more insights (Table E3 [online]), despite being limited to Medtronic devices. Most of these studies were conducted between 2005 and 2011, coinciding with the Food and Drug Administration warning release and archiving regarding DBS MRI safety (6). The majority performed MRI in patients in accordance with DBS vendor guidelines, presumably with the intent of confirming the safety of said guidelines. Tagliati et al (11) reported no adverse events in more than 3000 patients with DBS scanned at 1.5 T (although one center used 1.0 T). Furthermore, no studies listed in Table E3 (online) reported adverse events. However, some studies used MRI parameters outside of DBS vendor guidelines, using sequences with high SAR (22,70,71), atypical IPG placement (such as in the abdomen) (72), or higher field strength (ie, 3.0 T) (12,16,40,73). Studies performing 3.0-T MRI reported no adverse events in 88 patients (16,40,64,73,74), among which 27 were performed with a body-transmit coil. Furthermore, the extent of the MRI artifact related to the DBS device was also limited on functional MRI sequences (Figs 4, 5) (73). Thus far, most functional MRI studies in patients with DBS have been limited to 1.5 T (19,75–80). The possibility of acquiring data—in particular, functional MRI—with optimal MRI hardware in patients with DBS may not only help to expand clinical MRI applications, but also could

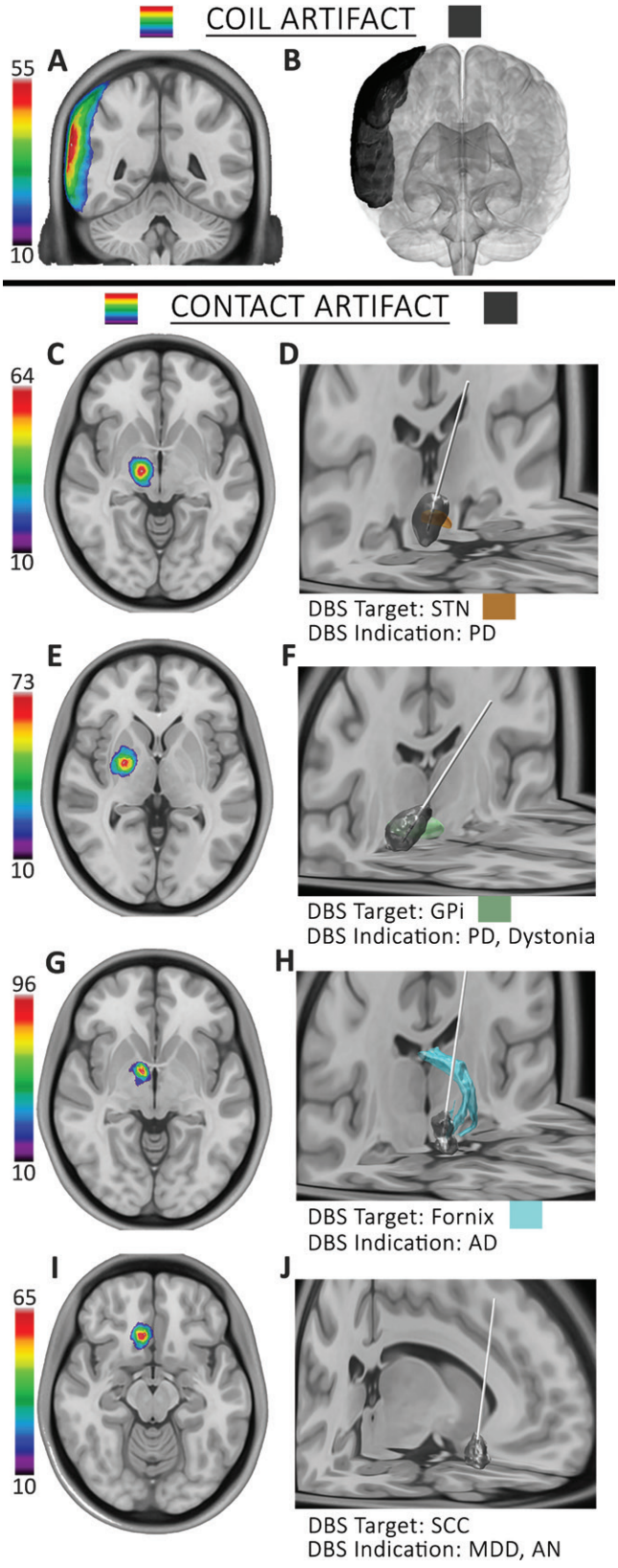

Figure 5: Images show deep brain stimulation (DBS) artifact distributions. DBS hardware artifact probability maps for, *A, B,* coil artifact and, *C–J,* DBS electrode contacts included in study cohort. For group analysis, individual participant's coil and electrode contact artifacts were transformed (ie, normalized) to standard brain (Montreal Neurological Institute [MNI] brain). Left-sided artifacts were flipped on right side. Artifact frequency maps were then obtained by summing artifacts and then dividing by size of each group (color bar unit equals percentage). *A, C, E, G, I,* Two-dimensional frequency maps are shown on axial T1-weighted images from MRI of brain. Frequency maps were thresholded at 10% (ie, these voxels were only shadowed in 10% of participants) for visualization. Right and left images follow radiologic conventions. *B, D, F, H, J,* Three-dimensional reconstructions of frequency maps are shown in T1-weighted MNI brain image with relevant DBS target. Three-dimensional visualization of DBS targets was performed with Lead-DBS toolbox (*https://www.lead-dbs.org*). Anterior thalamic nucleus contact artifact map was not included because it applied to only one participant. AD = Alzheimer disease, AN = anorexia nervosa, GPi = globus pallidus interna, MDD = major depressive disorder, PD = Parkinson disease, SCC = subcallosal cingulate cortex, STN = subthalamic nucleus. (Reprinted, with permission, from reference 73.)

facilitate important discoveries in the field of neuromodulation. Given the constant evolution of MRI systems and DBS devices, it is difficult to differentiate between inherent risks and lack of safety testing by the implant manufacturer. As with most aspects of medicine, clinicians should always weigh the advantages and disadvantages of a diagnostic test. If the MRI is likely to provide substantial benefits for the patient with DBS, then some degree of risk may be acceptable (81).

Studies reported IPG dysfunction (absent of patient injuries) in older IPG models, most commonly the Itrel model (Medtronic) (54,72,82) and noting spontaneous activation or deactivation of IPG. Magnet-related activation of IPG reportedly occurred spontaneously during MRI, up to 427 times during a single MRI session (54). In rare instances, it required the replacement of IPG (11). Although more recent studies have not specifically assessed IPG output, the lack of reported adverse effects or changes in patients' clinical status is reassuring and suggests modern IPG output is stable during MRI (12,16,40,73). Nevertheless, IPG status should be routinely checked after MRI. Stability of the DBS device impedances ensure the electrical circuit integrity of the system and the stability of peri-electrode tissue (eg, absence of gross edema or hemorrhage) (12,73). Finally, few recent studies explicitly report performing MRI while modern IPGs were turned on using patients' optimal stimulation settings, most often monopolar stimulation (12,16,73). At present, only one vendor allows IPG to be turned on to bipolar stimulation during MRI (9). This is problematic because turning off the IPG or using suboptimal settings typically exacerbates patients' symptoms. Clarifying the safety and stability of IPG output requires further studies, regardless of current type.

Techniques and Tools to Improve Safety

Technologic advancements create opportunities to use techniques and tools to improve MRI safety for patients with DBS (Table 2). Since the Food and Drug Administration warning was archived in 2011, a dramatic increase in studies report innovative ways to improve MRI safety for patients with neurostimulators (Fig 1).

Table 2 categorizes technique and tool-related studies into optimized MRI acquisition parameters, DBS hardware modification, MRI hardware (including coils), and simulation models (Table 2). Few studies aim to change DBS device design, possibly due to the proprietary nature of medical devices and the technologic and economic barriers precluding

Table 2: Techniques and Tools to Improve MRI Safety

Study	Category	Summary Findings
Sarkar et al, 2014 (92); Sarkar et al, 2014 (93); Sarkar et al, 2014 (94)	MRI acquisition parameters	Routine clinical sequence (eg, STIR) modified to a low SAR version (eg, decreased scan averages) while maintaining tissue contrast and clinically feasible acquisition times
Elwassif et al, 2012 (83)	DBS hardware	Electrode with a heat sink (change of the insulation material) to decrease heating
Serano et al, 2015 (112)	DBS hardware	Electrode with a resistive tapered stripline design (ie, stripline-based design to scatter the RF energy) to decrease SAR and heating
Golestanirad et al, 2019 (113)	DBS hardware	Electrode with thin layer of high dielectric constant material coat to decrease SAR and heating
Eryaman et al, 2015 (114); Gudino et al, 2015 (115); McElcheran et al, 2015 (89); McElcheran et al, 2017 (90); Eryaman et al, 2019 (116); Guerin et al, 2019 (91); McElcheran et al, 2019 (88)	MRI hardware and coil	Parallel RF transmit to minimize SAR and heating
Golestanirad et al, 2017 (86); Golestanirad et al, 2017 (87); Golestanirad et al, 2019 (117); Kazemivalipour et al, 2019 (118)	MRI hardware and coil	Patient-adjustable reconfigurable coil (ie, rotatable linearly polarized birdcage transmitter) to minimize SAR and heating
Golestanirad et al, 2019 (119)	MRI hardware and coil	High−field vertical scanners to minimize SAR
Golombeck et al, 2002 (96)	Simulation models	Thermodynamic algorithm to estimate heating
Angelone et al, 2010 (120)	Simulation models	Computational model aiming at balancing the requirements of SAR deposition at the tip of the lead and power dissipation of the device battery
Iacono et al, 2013 (100)	Simulation models	Numerical modeling of the RF field in patients with DBS by using MRI anatomic details
Bonmassar et al, 2014 (99)	Simulation models	MRI-based virtual patient simulator to enable estimation of safety parameters (eg, SAR), to improve RF power dosimetry, and to evaluate the effect of different lead pathway and MRI technology
Guerin et al, 2018 (98)	Simulation models	CT-based virtual patient simulator to enable estimation of SAR
Golestanirad et al, 2019 (101)	Simulation models	CT-based computation modeling of SAR and heating, which also assesses DBS device configuration influence

Note.—DBS = deep brain stimulation, RF = radiofrequency, SAR = specific absorption rate, STIR = short inversion time inversion-recovery.

most researchers from building in-house devices. For example, Elwassif et al (83) incorporated device components to act as heat sinks (ie, modification of the thermal conductivity of support material), which can disperse potentially hazardous temperature rises. In addition to safety considerations, DBS electrode design may undergo modification to decrease the MRI-related susceptibility artifact (84,85). Other studies have reported MRI hardware and coil modifications to improve MRI safety. Given the influence of the spatial relationship between MRI coils and the DBS device, investigators have developed modified coils resulting in lower SAR and heating, specifically proposing the use of a rotatable linearly polarized birdcage transmitter (86,87) and an optimized parallel RF transmission with a different coil design (88–91). One group dedicated their efforts into customizing MRI acquisition parameters to limit the use of RF pulses—and thus SAR—while maintaining image quality (92–94). Finally, computational models provide an opportunity to explore the multivariable problem of RF-associated heating and further elucidate the interaction between electromagnetic fields and biologic tissues (95,96). Generally, these studies aim to either provide tools that computationally simulate and estimate temperature rise at the electrode or establish a means through which to minimize DBS device heating on an individual patient basis. Individualized models of patients with DBS (97–99), high-spatial-resolution anatomic templates (100), and the angle of DBS lead insertion (101) have been investigated with computerized simulation. However, these tools require further studies to confirm their reliability in maintaining patient safety.

Summary of Best Practice Guidelines for Imaging Patients with DBS

Patients with DBS devices commonly present for MRI examinations. Fortunately, newer DBS devices have less restrictive MRI guidelines and more practical vendor specifications. However, radiologists commonly have requests for MRI examinations outside of the labeling requirements of a specific DBS device. In these circumstances, the clinician must determine whether (and how) to proceed with the

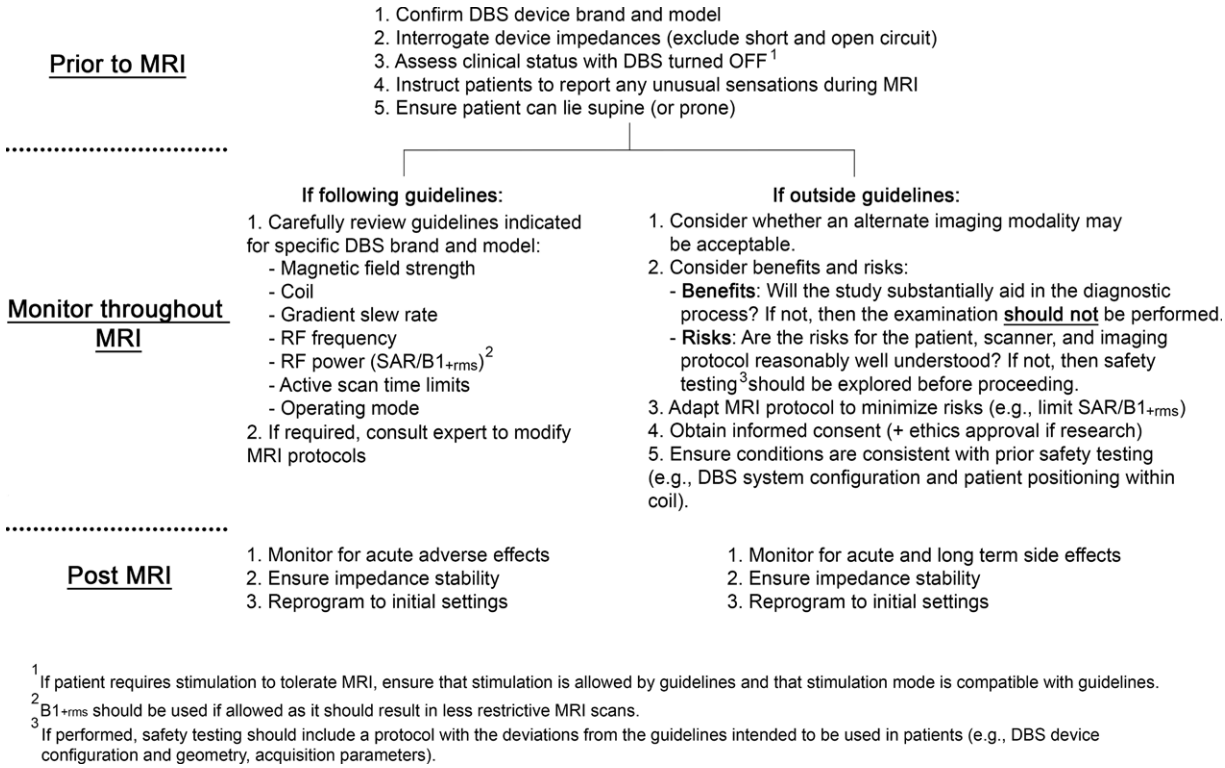

[1] If patient requires stimulation to tolerate MRI, ensure that stimulation is allowed by guidelines and that stimulation mode is compatible with guidelines.
[2] B1+rms should be used if allowed as it should result in less restrictive MRI scans.
[3] If performed, safety testing should include a protocol with the deviations from the guidelines intended to be used in patients (e.g., DBS device configuration and geometry, acquisition parameters).

Figure 6: Image shows summary recommendations of best practices for MRI in patients with deep brain stimulation (DBS) devices. These recommendations are based on guidelines of DBS vendors, literature reviewed herein, and authors' own experience. Recommendations for performing safety testing can be found in American Society for Testing and Materials International, International Organization for Standardization Technical Standard 10974, and other documents. B_{1+RMS} = root-mean-square value of MRI effective component of RF magnetic (B_1) field, RF = radiofrequency, SAR = specific absorption rate. Source.—References 8–10, 25, 28, 29.

MRI examination. Based on the guidelines of DBS vendors (8–10), reviewed literature, and our experience, we include a summary of recommendations of best practices for MRI in patients with DBS devices (Fig 6). These recommendations are not intended to account for all circumstances but provide a framework through which radiology groups can approach MRI in patients with DBS devices.

Future Directions

Heating remains the primary risk associated with DBS devices. This requires an accurate and reliable way to predict implant heating, rather than simply providing whole-body measures of heating, such as SAR or B_{1+RMS} (32,42,99).

In the future, institutions that adopt patient-specific computerized models could then be applied in simulation software (102). The simulation tools currently under development align with providing individualized safety risks (97–99). If needed, then radiologists could modify routinely used protocols to remain within the safe limits determined by the bespoke simulation software, rather than limiting patients to the same MRI field strengths and low-SAR pulse sequences as if they were a homogeneous group.

Lowering the risk of heating altogether is not an easy task, as it would primarily involve changing the design of DBS devices and minimizing wire length. Drastic reductions in heating could potentially be achieved with technologic advancements such as much smaller, cranially placed IPG or wireless electrodes (103,104).

Finally, MRI safety advances in patients with DBS have opened research possibilities. Specifically, prospective acquisition of suboptimal functional MRI data (ie, 1.5 T, head-transmit coil) in patients with Parkinson disease and DBS showed promise as a marker of efficacy, suggesting that state-of-the-art functional neuroimaging data (ie, 3.0 T, body-transmit coil) may potentially represent an unparalleled research tool to probe brain functions. The risks of DBS devices in ultra-high-field-strength MRI (ie, 7.0 T) remains unevaluated (105). However, investigating the safety of ultra-high-field-strength MRI in patients with DBS is garnering interest because of its potential to be used as a powerful research and clinical tool.

Conclusion

Following MRI-related patient injuries in the early 2000s, considerable efforts have been made by both vendors and the scientific community to advance our understanding of deep brain stimulation (DBS) device and MRI safety and to provide further safeguards. Notably, heating remains a serious issue when venturing outside the prescribed guidelines.

At present, investigators are using innovative methods, particularly computational models, to assess MRI safety of neurostimulators in a more comprehensive and generalizable manner. Tailoring MRI safety guidelines to the individual may be the sensible next step for realizing the full potential of MRI in patients with a DBS device.

Acknowledgments: We would like to thank our illustrator, Andrew O'Connor, BA, for helping with the design of Figure 2.

Disclosures of Conflicts of Interest: **A.B.** disclosed no relevant relationships. **C.T.C.** disclosed no relevant relationships. **K.N.** disclosed no relevant relationships. **G.J.B.E.** disclosed no relevant relationships. **C.N.** disclosed no relevant relationships. **J.G.** disclosed no relevant relationships. **M.R.** disclosed no relevant relationships. **A.L.** disclosed no relevant relationships. **A.J.M.** Activities related to the present article: disclosed no relevant relationships. Activities not related to the present article: has grants/grants pending for MRI interventions (ClearPoint Neuro); is a consultant for UniQure. Other relationships: disclosed no relevant relationships. **W.K.** Activities related to the present article: disclosed no relevant relationships. Activities not related to the present article: is employed by the University of Toronto. Other relationships: disclosed no relevant relationships. **C.J.S.** disclosed no relevant relationships. **I.H.** Activities related to the present article: disclosed no relevant relationships. Activities not related to the present article: was employed by General Electric; is employed by the National Institutes of Health. Other relationships: disclosed no relevant relationships. **A.R.R.** disclosed no relevant relationships. **A.M.L.** Activities related to the present article: disclosed no relevant relationships. Activities not related to the present article: is a consultant for Abbott, Boston Scientific, Functional Neuromodulation, and Medtronic. Other relationships: disclosed no relevant relationships.

References

1. Lozano AM, Lipsman N. Probing and regulating dysfunctional circuits using deep brain stimulation. Neuron 2013;77(3):406–424.
2. Lozano AM, Lipsman N, Bergman H, et al. Deep brain stimulation: current challenges and future directions. Nat Rev Neurol 2019;15(3):148–160.
3. Hariz M. My 25 Stimulating Years with DBS in Parkinson's Disease. J Parkinsons Dis 2017;7(s1):S33–S41.
4. Falowski S, Safriel Y, Ryan MP, Hargens L. The Rate of Magnetic Resonance Imaging in Patients with Deep Brain Stimulation. Stereotact Funct Neurosurg 2016;94(3):147–153.
5. Oluigbo CO, Rezai AR. Magnetic resonance imaging safety of deep brain stimulator devices. Handb Clin Neurol 2013;116:73–76.
6. Gupte AA, Shrivastava D, Spaniol MA, Abosch A. MRI-related heating near deep brain stimulation electrodes: more data are needed. Stereotact Funct Neurosurg 2011;89(3):131–140.
7. Baker KB, Tkach JA, Nyenhuis JA, et al. Evaluation of specific absorption rate as a dosimeter of MRI-related implant heating. J Magn Reson Imaging 2004;20(2):315–320.
8. Boston Scientific. ImageReady MRI Guidelines for Boston Scientific Deep Brain Stimulation Systems. Boston, Mass: Boston Scientific, 2017; 613.
9. Medtronic. MRI guidelines for Medtronic deep brain stimulation systems. Dublin, Ireland: Medtronic, 2015; 44.
10. St. Jude Medical. MRI procedure information for St. Jude Medical MR conditional deep brain stimulation systems. Saint Paul, Minn: St. Jude Medical, 2018; 23.
11. Tagliati M, Jankovic J, Pagan F, et al. Safety of MRI in patients with implanted deep brain stimulation devices. Neuroimage 2009;47(Suppl 2):T53–T57.
12. Boutet A, Hancu I, Saha U, et al. 3-Tesla MRI of deep brain stimulation patients: safety assessment of coils and pulse sequences. J Neurosurg 2019 Feb 22:1–9 [Epub ahead of print].
13. Kraff O, Quick HH. 7T: Physics, safety, and potential clinical applications. J Magn Reson Imaging 2017;46(6):1573–1589.
14. Dula AN, Virostko J, Shellock FG. Assessment of MRI issues at 7 T for 28 implants and other objects. AJR Am J Roentgenol 2014;202(2):401–405.
15. Feng DX, McCauley JP, Morgan-Curtis FK, et al. Evaluation of 39 medical implants at 7.0 T. Br J Radiol 2015;88(1056):20150633.
16. Hancu I, Boutet A, Fiveland E, et al. On the (Non-)equivalency of monopolar and bipolar settings for deep brain stimulation fMRI studies of Parkinson's disease patients. J Magn Reson Imaging 2019;49(6):1736–1749.
17. Horn A, Wenzel G, Irmen F, et al. Deep brain stimulation induced normalization of the human functional connectome in Parkinson's disease. Brain 2019;142(10):3129–3143.
18. Hiss S, Hesselmann V, Hunsche S, et al. Intraoperative functional magnetic resonance imaging for monitoring the effect of deep brain stimulation in patients with obsessive-compulsive disorder. Stereotact Funct Neurosurg 2015;93(1):30–37.
19. Stefurak T, Mikulis D, Mayberg H, et al. Deep brain stimulation for Parkinson's disease dissociates mood and motor circuits: a functional MRI case study. Mov Disord 2003;18(12):1508–1516.
20. Tae WS, Ham BJ, Pyun SB, Kang SH, Kim BJ. Current Clinical Applications of Diffusion-Tensor Imaging in Neurological Disorders. J Clin Neurol 2018;14(2):129–140.
21. Drake-Pérez M, Boto J, Fitsiori A, Lovblad K, Vargas MI. Clinical applications of diffusion weighted imaging in neuroradiology. Insights Imaging 2018;9(4):535–547.
22. Larson PS, Richardson RM, Starr PA, Martin AJ. Magnetic resonance imaging of implanted deep brain stimulators: experience in a large series. Stereotact Funct Neurosurg 2008;86(2):92–100.
23. Bronstein JM, Tagliati M, Alterman RL, et al. Deep brain stimulation for Parkinson disease: an expert consensus and review of key issues. Arch Neurol 2011;68(2):165.
24. Dormont D, Seidenwurm D, Galanaud D, Cornu P, Yelnik J, Bardinet E. Neuroimaging and deep brain stimulation. AJNR Am J Neuroradiol 2010;31(1):15–23.
25. American Society for Testing and Materials (ASTM). F2182-11a, Standard Test Method for Measurement of Radio Frequency Induced Heating On or Near Passive Implants During Magnetic Resonance Imaging. West Conshohocken, Pa: ASTM International, 2011.
26. Erhardt JB, Fuhrer E, Gruschke OG, et al. Should patients with brain implants undergo MRI? J Neural Eng 2018;15(4):041002.
27. Delfino JG, Woods TO. New Developments in Standards for MRI Safety Testing of Medical Devices. Curr Radiol Rep 2016;4(6):28.
28. International Organization for Standardization Technical Standard (ISO/TS). 10974/Ed. 2, Assessment of the safety of magnetic resonance imaging for patients with an active implantable medical device. Report No. ISO/TS 10974:2018(E). Geneva, Switzerland: International Organization for Standardization, 2018.
29. International Electrotechnical Commission (IEC). 60601-2-33, Medical electrical equipment - Part 2-33: Particular requirements for the basic safety and essential performance of magnetic resonance equipment for medical diagnosis. Geneva, Switzerland: IEC, 2010.
30. Rezai AR, Phillips M, Baker KB, et al. Neurostimulation system used for deep brain stimulation (DBS): MR safety issues and implications of failing to follow safety recommendations. Invest Radiol 2004;39(5):300–303.
31. Shellock FG. Magnetic resonance safety update 2002: implants and devices. J Magn Reson Imaging 2002;16(5):485–496.
32. Rezai AR, Baker KB, Tkach JA, et al. Is magnetic resonance imaging safe for patients with neurostimulation systems used for deep brain stimulation? Neurosurgery 2005;57(5):1056–1062; discussion 1056–1062.
33. Rezai AR, Finelli D, Nyenhuis JA, et al. Neurostimulation systems for deep brain stimulation: in vitro evaluation of magnetic resonance imaging-related heating at 1.5 tesla. J Magn Reson Imaging 2002;15(3):241–250.
34. Konings MK, Bartels LW, Smits HF, Bakker CJ. Heating around intravascular guidewires by resonating RF waves. J Magn Reson Imaging 2000;12(1):79–85.
35. Georgi JC, Stippich C, Tronnier VM, Heiland S. Active deep brain stimulation during MRI: a feasibility study. Magn Reson Med 2004;51(2):380–388.
36. Liu CY, Farahani K, Lu DS, Duckwiler G, Oppelt A. Safety of MRI-guided endovascular guidewire applications. J Magn Reson Imaging 2000;12(1):75–78.
37. Bhidayasiri R, Bronstein JM, Sinha S, et al. Bilateral neurostimulation systems used for deep brain stimulation: in vitro study of MRI-related heating at 1.5 T and implications for clinical imaging of the brain. Magn Reson Imaging 2005;23(4):549–555.
38. Finelli DA, Rezai AR, Ruggieri PM, et al. MR imaging-related heating of deep brain stimulation electrodes: in vitro study. AJNR Am J Neuroradiol 2002;23(10):1795–1802.
39. Kahan J, Papadaki A, White M, et al. The Safety of Using Body-Transmit MRI in Patients with Implanted Deep Brain Stimulation Devices. PLoS One 2015;10(6):e0129077.
40. Sammartino F, Krishna V, Sankar T, et al. 3-Tesla MRI in patients with fully implanted deep brain stimulation devices: a preliminary study in 10 patients. J Neurosurg 2017;127(4):892–898.
41. Yablonskiy DA, Ackerman JJ, Raichle ME. Coupling between changes in human brain temperature and oxidative metabolism during prolonged visual stimulation. Proc Natl Acad Sci U S A 2000;97(13):7603–7608 [Published correction appears in Proc Natl Acad Sci U S A 2000;97(17):9819.].
42. Kainz W. MR heating tests of MR critical implants. J Magn Reson Imaging 2007;26(3):450–451.
43. Calcagnini G, Triventi M, Censi F, et al. In vitro investigation of pacemaker lead heating induced by magnetic resonance imaging: role of implant geometry. J Magn Reson Imaging 2008;28(4):879–886.
44. Baker KB, Tkach JA, Phillips MD, Rezai AR. Variability in RF-induced heating of a deep brain stimulation implant across MR systems. J Magn Reson Imaging 2006;24(6):1236–1242.
45. Shellock FG. Comments on MR heating tests of critical implants. J Magn Reson Imaging 2007;26(5):1182–1185.

46. Nordbeck P, Weiss I, Ehses P, et al. Measuring RF-induced currents inside implants: Impact of device configuration on MRI safety of cardiac pacemaker leads. Magn Reson Med 2009;61(3):570–578.
47. Qian D, El-Sharkawy AM, Bottomley PA, Edelstein WA. An RF dosimeter for independent SAR measurement in MRI scanners. Med Phys 2013;40(12):122303.
48. Rezai AR, Finelli D, Rugieri P, Tkach J, Nyenhuis JA, Shellock FG. Neurostimulators: potential for excessive heating of deep brain stimulation electrodes during magnetic resonance imaging. J Magn Reson Imaging 2001;14(4):488–489.
49. Allison J, Yanasak N. What MRI Sequences Produce the Highest Specific Absorption Rate (SAR), and Is There Something We Should Be Doing to Reduce the SAR During Standard Examinations? AJR Am J Roentgenol 2015;205(2):W140.
50. Schmitz BL, Aschoff AJ, Hoffmann MH, Grön G. Advantages and pitfalls in 3T MR brain imaging: a pictorial review. AJNR Am J Neuroradiol 2005;26(9):2229–2237.
51. Carmichael DW, Pinto S, Limousin-Dowsey P, et al. Functional MRI with active, fully implanted, deep brain stimulation systems: safety and experimental confounds. Neuroimage 2007;37(2):508–517.
52. Boutet A, Jain M, Elias GJB, et al. Network Basis of Seizures Induced by Deep Brain Stimulation: Literature Review and Connectivity Analysis. World Neurosurg 2019;132:314–320.
53. Gleason CA, Kaula NF, Hricak H, Schmidt RA, Tanagho EA. The effect of magnetic resonance imagers on implanted neurostimulators. Pacing Clin Electrophysiol 1992;15(1):81–94.
54. Tronnier VM, Staubert A, Hähnel S, Sarem-Aslani A. Magnetic resonance imaging with implanted neurostimulators: an in vitro and in vivo study. Neurosurgery 1999;44(1):118–125; discussion 125–126.
55. Medtronic. DBS™ 37086 extension kit for deep brain stimulation (8-4). Minneapolis, Minn: Medtronic, 2016.
56. Medtronic. DBS™ 3387, 3389 lead kit for deep brain stimulation. Minneapolis, Minn: Medtronic, 2017.
57. Medtronic. Activa® PC 37601 Multi-program neurostimulator. Minneapolis, Minn: Medtronic, 2010.
58. Cabot E, Lloyd T, Christ A, et al. Evaluation of the RF heating of a generic deep brain stimulator exposed in 1.5 T magnetic resonance scanners. Bioelectromagnetics 2013;34(2):104–113.
59. Park SM, Nyenhuis JA, Smith CD, et al. Gelled versus nongelled phantom material for measurement of MRI-induced temperature increases with bioimplants. IEEE Trans Magn 2003;39(5):3367–3371.
60. Hartsgrove G, Kraszewski A, Surowiec A. Simulated biological materials for electromagnetic radiation absorption studies. Bioelectromagnetics 1987;8(1):29–36.
61. Kainz W, Neubauer G, Uberbacher R, Alesch F, Chan DD. Temperature measurement on neurological pulse generators during MR scans. Biomed Eng Online 2002;1(1):2.
62. Nazzaro JM, Klemp JA, Brooks WM, et al. Deep brain stimulation lead-contact heating during 3T MRI: single- versus dual-channel pulse generator configurations. Int J Neurosci 2014;124(3):166–174.
63. Baker KB, Nyenhuis JA, Hrdlicka G, Rezai AR, Tkach JA, Shellock FG. Neurostimulation systems: assessment of magnetic field interactions associated with 1.5- and 3-Tesla MR systems. J Magn Reson Imaging 2005;21(1):72–77.
64. Phillips MD, Baker KB, Lowe MJ, et al. Parkinson disease: pattern of functional MR imaging activation during deep brain stimulation of subthalamic nucleus--initial experience. Radiology 2006;239(1):209–216.
65. Schueler BA, Parrish TB, Lin JC, et al. MRI compatibility and visibility assessment of implantable medical devices. J Magn Reson Imaging 1999;9(4):596–603.
66. Baker KB, Tkach J, Hall JD, Nyenhuis JA, Shellock FG, Rezai AR. Reduction of magnetic resonance imaging-related heating in deep brain stimulation leads using a lead management device. Neurosurgery 2005;57(4 Suppl):392–397; discussion 392–397.
67. Mayberg HS, Lozano AM, Voon V, et al. Deep brain stimulation for treatment-resistant depression. Neuron 2005;45(5):651–660.
68. Shrivastava D, Abosch A, Hanson T, et al. Effect of the extracranial deep brain stimulation lead on radiofrequency heating at 9.4 Tesla (400.2 MHz). J Magn Reson Imaging 2010;32(3):600–607.
69. Shrivastava D, Abosch A, Hughes J, et al. Heating induced near deep brain stimulation lead electrodes during magnetic resonance imaging with a 3 T transceive volume head coil. Phys Med Biol 2012;57(17):5651–5665.
70. Chhabra V, Sung E, Mewes K, Bakay RA, Abosch A, Gross RE. Safety of magnetic resonance imaging of deep brain stimulator systems: a serial imaging and clinical retrospective study. J Neurosurg 2010;112(3):497–502.
71. Fraix V, Chabardes S, Krainik A, et al. Effects of magnetic resonance imaging in patients with implanted deep brain stimulation systems. J Neurosurg 2010;113(6):1242–1245.
72. Nazzaro JM, Lyons KE, Wetzel LH, Pahwa R. Use of brain MRI after deep brain stimulation hardware implantation. Int J Neurosci 2010;120(3):176–183.
73. Boutet A, Rashid T, Hancu I, et al. Functional MRI Safety and Artifacts during Deep Brain Stimulation: Experience in 102 Patients. Radiology 2019;293(1):174–183.
74. DiMarzio M, Rashid T, Hancu I, et al. Functional MRI Signature of Chronic Pain Relief From Deep Brain Stimulation in Parkinson Disease Patients. Neurosurgery 2019;85(6):E1043–E1049.
75. Hesselmann V, Sorger B, Girnus R, et al. Intraoperative functional MRI as a new approach to monitor deep brain stimulation in Parkinson's disease. Eur Radiol 2004;14(4):686–690.
76. Jech R, Mueller K, Urgošík D, et al. The subthalamic microlesion story in Parkinson's disease: electrode insertion-related motor improvement with relative cortico-subcortical hypoactivation in fMRI. PLoS One 2012;7(11):e49056.
77. Jech R, Urgosík D, Tintera J, et al. Functional magnetic resonance imaging during deep brain stimulation: a pilot study in four patients with Parkinson's disease. Mov Disord 2001;16(6):1126–1132.
78. Kahan J, Urner M, Moran R, et al. Resting state functional MRI in Parkinson's disease: the impact of deep brain stimulation on 'effective' connectivity. Brain 2014;137(Pt 4):1130–1144.
79. Knight EJ, Testini P, Min HK, et al. Motor and Nonmotor Circuitry Activation Induced by Subthalamic Nucleus Deep Brain Stimulation in Patients With Parkinson Disease: Intraoperative Functional Magnetic Resonance Imaging for Deep Brain Stimulation. Mayo Clin Proc 2015;90(6):773–785.
80. Mueller K, Jech R, Schroeter ML. Deep-brain stimulation for Parkinson's disease. N Engl J Med 2013;368(5):482–483.
81. Martin AJ. MRI in Patients with Deep Brain Stimulation Electrodes: Balancing Risks and Benefits. Radiology 2019;293(1):184–185.
82. Rezai AR, Lozano AM, Crawley AP, et al. Thalamic stimulation and functional magnetic resonance imaging: localization of cortical and subcortical activation with implanted electrodes. Technical note. J Neurosurg 1999;90(3):583–590.
83. Elwassif MM, Datta A, Rahman A, Bikson M. Temperature control at DBS electrodes using a heat sink: experimentally validated FEM model of DBS lead architecture. J Neural Eng 2012;9(4):046009.
84. Lai HY, Albaugh DL, Kao YC, Younce JR, Shih YY. Robust deep brain stimulation functional MRI procedures in rats and mice using an MR-compatible tungsten microwire electrode. Magn Reson Med 2015;73(3):1246–1251.
85. Zhao S, Liu X, Xu Z, et al. Graphene Encapsulated Copper Microwires as Highly MRI Compatible Neural Electrodes. Nano Lett 2016;16(12):7731–7738.
86. Golestanirad L, Iacono MI, Keil B, et al. Construction and modeling of a reconfigurable MRI coil for lowering SAR in patients with deep brain stimulation implants. Neuroimage 2017;147:577–588.
87. Golestanirad L, Keil B, Angelone LM, Bonmassar G, Mareyam A, Wald LL. Feasibility of using linearly polarized rotating birdcage transmitters and close-fitting receive arrays in MRI to reduce SAR in the vicinity of deep brain simulation implants. Magn Reson Med 2017;77(4):1701–1712.
88. McElcheran CE, Golestanirad L, Iacono MI, et al. Numerical Simulations of Realistic Lead Trajectories and an Experimental Verification Support the Efficacy of Parallel Radiofrequency Transmission to Reduce Heating of Deep Brain Stimulation Implants during MRI. Sci Rep 2019;9(1):2124.
89. McElcheran CE, Yang B, Anderson KJ, Golenstani-Rad L, Graham SJ. Investigation of Parallel Radiofrequency Transmission for the Reduction of Heating in Long Conductive Leads in 3 Tesla Magnetic Resonance Imaging. PLoS One 2015;10(8):e0134379.
90. McElcheran CE, Yang B, Anderson KJT, Golestanirad L, Graham SJ. Parallel radiofrequency transmission at 3 tesla to improve safety in bilateral implanted wires in a heterogeneous model. Magn Reson Med 2017;78(6):2406–2415.
91. Guerin B, Angelone LM, Dougherty D, Wald LL. Parallel transmission to reduce absorbed power around deep brain stimulation devices in MRI: Impact of number and arrangement of transmit channels. Magn Reson Med 2020;83(1):299–311.
92. Sarkar SN, Papavassiliou E, Hackney DB, et al. Three-dimensional brain MRI for DBS patients within ultra-low radiofrequency power limits. Mov Disord 2014;29(4):546–549.
93. Sarkar SN, Papavassiliou E, Rojas R, et al. Low-power inversion recovery MRI preserves brain tissue contrast for patients with Parkinson disease with deep brain stimulators. AJNR Am J Neuroradiol 2014;35(7):1325–1329.
94. Sarkar SN, Sarkar PR, Papavassiliou E, Rojas RR. Utilizing fast spin echo MRI to reduce image artifacts and improve implant/tissue interface detection in refractory Parkinson's patients with deep brain stimulators. Parkinsons Dis 2014;2014:508576.
95. Griffin GH, Anderson KJ, Celik H, Wright GA. Safely assessing radiofrequency heating potential of conductive devices using image-based current measurements. Magn Reson Med 2015;73(1):427–441.

96. Golombeck MA, Thiele J, Dössel O. Magnetic resonance imaging with implanted neurostimulators: numerical calculation of the induced heating. Biomed Tech (Berl) 2002;47(Suppl 1 Pt 2):660–663.
97. Guerin B, Iacono MI, Davids M, Dougherty D, Angelone LM, Wald LL. The 'virtual DBS population': five realistic computational models of deep brain stimulation patients for electromagnetic MR safety studies. Phys Med Biol 2019;64(3):035021.
98. Guerin B, Serano P, Iacono MI, et al. Realistic modeling of deep brain stimulation implants for electromagnetic MRI safety studies. Phys Med Biol 2018;63(9):095015.
99. Bonmassar G, Angelone LM, Makris N. A Virtual Patient Simulator Based on Human Connectome and 7 T MRI for Deep Brain Stimulation. Int J Adv Life Sci 2014;6(3-4):364–372.
100. Iacono MI, Makris N, Mainardi L, Angelone LM, Bonmassar G. MRI-based multiscale model for electromagnetic analysis in the human head with implanted DBS. Comput Math Methods Med 2013;2013:694171.
101. Golestanirad L, Kirsch J, Bonmassar G, et al. RF-induced heating in tissue near bilateral DBS implants during MRI at 1.5 T and 3T: The role of surgical lead management. Neuroimage 2019;184:566–576.
102. Kalloch B, Bode J, Kozlov M, et al. Semi-automated generation of individual computational models of the human head and torso from MR images. Magn Reson Med 2019;81(3):2090–2105.
103. Hosain MK, Kouzani AZ, Tye SJ, Abulseoud OA, Berk M. Design and analysis of an antenna for wireless energy harvesting in a head-mountable DBS device. Conf Proc IEEE Eng Med Biol Soc 2013;2013:3078–3081.
104. Alpaugh M, Saint-Pierre M, Dubois M, et al. A novel wireless brain stimulation device for long-term use in freely moving mice. Sci Rep 2019;9(1):6444.
105. Hoff MN, McKinney A 4th, Shellock FG, et al. Safety Considerations of 7-T MRI in Clinical Practice. Radiology 2019;292(3):509–518.
106. Nutt JG, Anderson VC, Peacock JH, Hammerstad JP, Burchiel KJ. DBS and diathermy interaction induces severe CNS damage. Neurology 2001;56(10):1384–1386.
107. Ruggera PS, Witters DM, von Maltzahn G, Bassen HI. In vitro assessment of tissue heating near metallic medical implants by exposure to pulsed radio frequency diathermy. Phys Med Biol 2003;48(17):2919–2928.
108. Food and Drug Administration (FDA) MAUDE Database 2001 FOI-TEXT2001A.ZIP, Report Number 330144. https://www.fda.gov/medical-devices/mandatory-reporting-requirements-manufacturers-importers-and-device-user-facilities/manufacturer-and-user-facility-device-experience-database-maude. Published March 30, 2001. Accessed July 23, 2019.
109. Spiegel J, Fuss G, Backens M, et al. Transient dystonia following magnetic resonance imaging in a patient with deep brain stimulation electrodes for the treatment of Parkinson disease. Case report. J Neurosurg 2003;99(4):772–774.
110. Henderson JM, Tkach J, Phillips M, Baker K, Shellock FG, Rezai AR. Permanent neurological deficit related to magnetic resonance imaging in a patient with implanted deep brain stimulation electrodes for Parkinson's disease: case report. Neurosurgery 2005;57(5):E1063; discussion E1063.
111. Zrinzo L, Yoshida F, Hariz MI, et al. Clinical safety of brain magnetic resonance imaging with implanted deep brain stimulation hardware: large case series and review of the literature. World Neurosurg 2011;76(1-2):164–172; discussion 69–73.
112. Serano P, Angelone LM, Katnani H, Eskandar E, Bonmassar G. A novel brain stimulation technology provides compatibility with MRI. Sci Rep 2015;5(1):9805.
113. Golestanirad L, Angelone LM, Kirsch J, et al. Reducing RF-induced Heating near Implanted Leads through High-Dielectric Capacitive Bleeding of Current (CBLOC). IEEE Trans Microw Theory Tech 2019;67(3):1265–1273.
114. Eryaman Y, Guerin B, Akgun C, et al. Parallel transmit pulse design for patients with deep brain stimulation implants. Magn Reson Med 2015;73(5):1896–1903.
115. Gudino N, Sonmez M, Yao Z, et al. Parallel transmit excitation at 1.5 T based on the minimization of a driving function for device heating. Med Phys 2015;42(1):359–371.
116. Eryaman Y, Kobayashi N, Moen S, et al. A simple geometric analysis method for measuring and mitigating RF induced currents on Deep Brain Stimulation leads by multichannel transmission/reception. Neuroimage 2019;184:658–668.
117. Golestanirad L, Kazemivalipour E, Keil B, et al. Reconfigurable MRI coil technology can substantially reduce RF heating of deep brain stimulation implants: First in-vitro study of RF heating reduction in bilateral DBS leads at 1.5 T. PLoS One 2019;14(8):e0220043.
118. Kazemivalipour E, Keil B, Vali A, et al. Reconfigurable MRI technology for low-SAR imaging of deep brain stimulation at 3T: Application in bilateral leads, fully-implanted systems, and surgically modified lead trajectories. Neuroimage 2019;199:18–29.
119. Golestanirad L, Kazemivalipour E, Lampman D, et al. RF heating of deep brain stimulation implants in open-bore vertical MRI systems: A simulation study with realistic device configurations. Magn Reson Med 2019 Nov 2 [Epub ahead of print].
120. Angelone LM, Ahveninen J, Belliveau JW, Bonmassar G. Analysis of the role of lead resistivity in specific absorption rate for deep brain stimulator leads at 3T MRI. IEEE Trans Med Imaging 2010;29(4):1029–1038.

10.1148/radiol.2020192291

Table E1. MRI safety studies with phantom models

Study	DBS Neurostimulators i. Brand ii. Lead model iii. Ext model iv. IPG model v. Rec model (if applicable)	Phantom Shape - Medium	MRI Hardware	MRI Coil	Experimental Design	Results
Gleason (1992) (53)	i. Medtronic ii. N/S iii. N/S iv. Itrel I v. 3360A, 7560A, 3464 i. Avery Laboratory ii. N/S iii. N/S iv. N/S v. Model 1 110A i. Cordis ii. N/S iii. N/S iv. MK II 904A	Cylinder Liquid (H_2O)	– 1.5T GE Signa IIs, (software N/S) – 0.35T Diasonics MT/S, (software N/S)	– Head-transmit – Body-transmit	Temperature elevations and DBS device movement with different field strengths. IPG output. DBS ON.	– Temperature increased up to 27°C rise at the IPG – IPG dysfunctions – Significant movement on IPG (Cordis)
Schueler (1999) (65)	i. Medtronic ii. 3387 iii. 7496 iv. Itrel II, Itrel III v. Xtrel, Mattrix receiver	Oval shoulders Semisolid ($NiSO_4$: 1.25 g/L)	– 1.5T Siemens Magnetom SP Vision	– Head-transmit/head-receive – Body-transmit/body-receive	Temperature elevations and DBS device movement. IPG output. DBS ON.	– No temperature rise. – No lead or IPG movement. – IPG dysfunctions.
Finelli (2002) (38)	i. Medtronic ii. 3387, 3389 iii. 7495 iv. Soletra	Head/torso Semisolid (PAA: 5.85 g/L)	– 1.5T Siemens Vision software v. Numaris 3.0, (model N/S)	– Head-transmit/head-receive	Temperature elevations with different pulse sequences.	– Temperature increased up to 6.7°C at the electrode tip when extension wire excess behind IPG (SAR 7.3 W/kg) – Largest temperature rise with the excess extension wire behind IPG
Kainz (2002) (61)	i. Medtronic ii. 3387 iii. N/S iv. Itrel 3	Head/torso Semisolid (ethylene glycol, natrium chloride)	– 1.5T Siemens Magnetom, (software N/S) – 3.0T Bruker BioPac, (software N/S)	– N/S	Temperature elevations with different field strengths. DBS OFF.	– Temperature increased up to 2.1°C at the electrode tips at 1.5T (SAR 2 W/kg) – Head MRI caused slightly more temperature increase than chest MRI – Temperature increases were similar for both 1.5T and 3.0T
Rezai (2002) (33)	i. Medtronic ii. 3387, 3389	Head/torso Semisolid (PAA:	– 1.5T Siemens Vision software v.	– Head-transmit/head-	Temperature elevations with	– Highest temperature elevations at the left electrode tips was 25.3°C when extension wire

	iii. 7495 iv. Soletra	5.85 g/L)	Numaris 3.0, (model N/S)	receive – Body-transmit/body-receive	different SAR, coils and DBS configurations. DBS OFF.	excess behind IPG (SAR = 12.2 W/kg) at the left electrode tips and with body-transmit coil. – Head-transmit coil caused less temperature rise (up to 7.1°C)
Park (2003) (59)	i. Medtronic ii. 3387 iii. 7495 iv. Soletra	Torso Semisolid (PAA: 0.7 g/L, 3.90 g/L, 5.85 g/L) or Liquid (H_2O)	– 1.5T GE Signa, (software N/S)	– Body-transmit	Temperature elevations with different phantom mediums.	– Temperature increased up to 16.2°C at the electrode tip (SAR 4.2 W/kg) – Greater temperature rise using PAA compared with saline solution
Baker (2004) (7)	i. Medtronic ii. 3387 iii. 7495 iv. Soletra	Head/torso Semisolid (con'c 5.85 g/L)	– 1.5T Siemens MR system 1 software Symphony v. Numaris 4 VA21B – 1.5T Siemens MR system 2 software Vision v. Numaris 3.0 VB33G	– Body-transmit/body-receive	Temperature elevations with different SAR.	– Different temperature increases per SAR values (ΔT/SAR) between MRI systems
Georgi (2004) (35)	i. Medtronic ii. 3387 iii. N/S iv. N/S	Head Liquid (NaCl or agar gel)	– 1.5T Siemens Symphony Quantum, (software N/S) – 2.35T Bruker BioSpec, (software N/S)	– Body-transmit	Temperature elevations and DBS device movement with different pulse sequences and DBS lead configurations. IPG output. DBS ON.	– Highest temperature elevations was 0.7°C for all pulse sequences (highest SAR = 0.92 W/kg) – No IPG dysfunction reported. – No noticeable movement of DBS lead. – Sparking observed when broken extension wire
Baker (2005) (66)	i. Medtronic ii. 3387–40 iii. 7495–51 iv. Soletra	Head Semisolid (PAA: 5.85 g/L)	– 1.5T Siemens Magnetom software Vision – 3.0T Siemens Magnetom software Allegra	– Body-transmit/body-receive – Head-transmit/head-receive	Temperature elevations with different DBS configurations.	– Concentric loops of extension wire around burr hole reduces heating
Bhidayasiri (2005) (37)	i. Medtronic ii. 3389 iii. 7495 iv. Soletra	Head/torso Semisolid (PAA: 5.85 g/L)	– 1.5T Siemens Sonata software Numaris/4 v. Syngo MR2002B	– Body-transmit/head-receive	Temperature elevations with different pulse sequences.	– Highest temperature elevations was 2.1°C for all pulse sequences (highest SAR = 2.9 W/kg)
Phillips (2006) (64)	i. Medtronic ii. 3387, 3389 iii. N/S iv. Soletra	Head/torso Semisolid (PAA: 5.85 g/L)	– 3.0T Siemens Allegra software Numaris Syngo v. VA21C	– N/S	Temperature elevations with different pulse sequences. DBS ON.	– Temperature elevations were < 1.4°C for all pulse sequences (highest SAR = 0.5 W/kg)
Baker (2006) (44)	i. Medtronic ii. 3387–40 iii. 7495–51 iv. Soletra	Head/torso Semisolid (PAA: 5.85 g/L)	– 1.5T Siemens MR system 1 software Symphony v. N4_VA25A – 1.5T Siemens MR system 2 software Avanto v. N4_VB11D	– Head-transmit/head-receive	Temperature elevations with different SAR. DBS OFF.	– Different temperature increases per SAR values (ΔT/SAR) between MRI systems
Carmichael (2007) (51)	i. Medtronic ii. 3389 iii. 7482 iv. Kinetra	Torso Semisolid (PAA: 8.0 g/L)	– 1.5T GE Signa Horizon LX Level 9.1 – 3.0T GE Excite Level 12 M4	– Head-transmit/head-receive	Temperature elevations with different field strengths. IPG output.	– Temperature elevations were higher with 3.0T (2.2°C, SAR = 2.3 W/kg) versus 1.5T (1.4°C, SAR = 1.5 W/kg) at the left electrode tip – IPG output stable

					DBS ON.	
Mohsin (2011) (121)	i. Medtronic ii. 3387, 3389 iii. N/S iv. N/S	N/S	– 1.5T, (brand, model, software N/S)	– Head-transmit/head-receive	Temperature elevations with different SAR and lead length.	– SAR highest around the electrode – SAR highest with longer lead
Nazzaro (2014) (62)	i. Medtronic ii. 3387 iii. 7482, 7482 iv. Soletra, Kinetra	Head/torso Semisolid (PAA)	– 3.0T Siemens Magnetom Allegra software 2004A	– Head-transmit/head-receive	Temperature elevations with single versus dual IPG.	– Temperature elevations were higher with bilateral (6.3°C) versus single IPG (3.8°C) – Temperature elevations higher at left electrode tip
Kahan (2015) (39)	i. Medtronic ii. 3389 iii. 37085 iv. Activa PC	Head/torso Semisolid (PAA: 8.0 g/L)	– 1.5T Siemens Magnetom Avanto software VB17 – 3.0T Siemens Tim Trio software VB17	– Head-transmit/body-receive – Body-transmit/head-receive	Temperature elevations with different field strengths and coils. IPG output. DBS ON.	– Temperature elevations were higher with body-transmit (1.3°C at 3.0T) versus head-transmit coil (1.4°C at 3.0T) – Temperature elevations were higher with 3.0T (1.4°C body coil) versus 1.5T (0.8°C body coil) – Phantom position relative to the body coil slightly impacted temperature elevations at 1.5T (< 1°C) – IPG output stable
Sammartino (2017) (40)	i. Medtronic ii. 3387 iii. 7482 iv. Soletra	Head/torso Semisolid (PAA: 8.0 g/L)	– 3.0T GE Signa software HDx v. 16.0 V02 1131.a	– Head-transmit/head-receive – Body-transmit/head-receive	Temperature elevations with different pulse sequences and coils. DBS OFF.	– Temperature elevations with clinical pulse sequences were < 1°C at the electrode tips with both coils.
Boutet (2019) (12)	i. Medtronic ii. 3387 iii. 37086 iv. Activa PC	Head/torso Semisolid (PAA: 8.0 g/L)	– 3.0T GE Signa software HDx v. 16.0 V02 1131.a	– Head-transmit/head-receive – Body-transmit/head-receive	Temperature elevations with different pulse sequences, coils and DBS configurations. IPG output. DBS ON.	– Temperature elevations with clinical pulse sequences were < 2°C at the electrode tips – Highest temperature elevation (6.4°C), SAR 2.1 = W/kg:B_{1+rms}=1.8μT) with unilateral DBS with loose side extensions – Temperature elevations similar for both coils – IPG output stable
Hancu (2019) (16)	i. Medtronic ii. 3387, 3389 iii. 37086 iv. Activa PC	Head/torso Semisolid (PAA: 10.02 g/L)	– 1.5T GE software HDx, (model N/S) – 3.0T GE Architect, (software N/S)	– Body-transmit/head-receive – Head-transmit/head-receive	Temperature elevations with different pulse sequences and DBS configurations. DBS ON.	– Temperature elevations with clinical pulse sequences were < 1°C using 3.0T body-transmit/head-receive – Highest temperature elevation (0.9°C), SAR = 1.3 W/kg/B_{1+rms}=2.6μT) – Temperature elevations with both configurations were < 1°C

Abbreviations: °C = Celsius, B_{1+rms} = root-mean-square value of the MRI effective component of the RF magnetic [B_1] field, DBS = deep brain stimulation, ext = extension, GE = General Electric, H_2O = distilled water, IPG = implantable pulse generator, kg = kilogram, L = liter, N/S = not specified, NaCl = sodium chloride, $NiSO_4$ = nickel sulfate, PAA = polyacrylic acid, Rec = receiver, SAR = specific absorption rate, SD = standard deviation, T = tesla, v. = version, W = watts, μ = micro.

Table E2. MRI safety studies with animals

Study	Animals	DBS Hardware i. Brand ii. Lead Model iii. Ext Model iv. IPG Model	MRI Hardware	MRI Coil	Experimental Design	Results
Shrivastava (2010) (122)	4 porcine heads	i. Medtronic ii. 3389 (externalized) iii. N/S iv. N/S	– No MRI used, only coil	– Head-transmit/head-receive	Temperature elevations with different orientations of extracranial portion of a DBS lead. DBS OFF.	– Temperature elevation up to 27°C (SAR = 2.94 W/kg) with perpendicular direction of the lead compared with 5°C (SAR = 2.94 W/kg) with axial direction at the electrode tips.
Shrivastava (2012) (69)	3 porcine heads	i. Medtronic ii. 3389 (externalized) iii. N/S iv. N/S	– 3.0T Siemens Trio (software N/S)	– Head-transmit/head-receive	Temperature elevations with different orientations of extracranial portion of a DBS lead. DBS OFF.	– Temperature elevation up to 24.7°C (SAR = 3.16 W/kg) with lateral lead loop compared with 3.2°C (SAR = 3.16 W/kg) with axial direction.
Gorny (2013) (123)	1 pig	i. Medtronic ii. 3389 iii. N/S iv. Soletra	– 1.5T/3.0T GE 14.0 M4 (software N/S)	– Head-transmit/head-receive	Temperature elevations with different pulse sequences. DBS ON/OFF.	– 3.0T MRI using GRE EPI and IR-FSPGR sequences (SAR = 0.41 W/kg/B_{1+rms} 0.30 uT and 0.49 W/kg/B_{1+rms} 1.09 uT, respectively) resulted in local temperature elevations at DBS electrodes of no more than 0.46°C
Shi (2014) (124)	48♂ rabbits	i. PINS Medical ii. Model G101 iii. Model G101 iv. Model G101	– 1.5T GE Signa HDxt GE software – 3.0T Siemens Verio Syngo software – 7.0T Bruker ClinScan, Syngo software	– Head-transmit/head-receive	Pathologic and molecular responses of brain tissue surrounding DBS leads, with different field strength. DBS OFF.	– No MRI-related detectable injury on brain tissue near DBS electrodes (1.5T, 3.0T, and 7.0T; SAR up to 2.96 W/kg)
Chen (2017) (125)	24♂ rabbits	i. PINS Medical ii. Model G101 iii. Model G101 iv. Model G101	– 1.5T GE Signa HDxt GE software – 3.0T Siemens Verio Syngo software – 7.0T Bruker ClinScan Syngo software	– N/S	Pathologic and molecular responses of brain tissue surrounding DBS leads, with different field strength.	– No MRI-related detectable injury on brain tissue near DBS electrodes (1.5T, 3.0T, and 7.0T; SAR up to 2.91 W/kg)

Abbreviations. ♂ = male, °C = Celsius, GE = General Electric, GRE-EPI = echo-planar imaging, IR-FSPGR = fast spoiled grass sequence with IR preparation, kg = kilograms, N/S = not specified, SAR = specific absorption rate, T = tesla, W = watts, μ = micro.

Table E3. MRI safety studies with participants

Study	No. Patients	DBS Hardware i. Brand ii. Lead Model iii. Ext Model iv. IPG Model	MRI Hardware	MRI Coil	Experimental Design	Results/Adverse Events
Rezai (1999) (82)	86	i. Medtronic ii. 3287 iii. N/S iv. Itrel II (externalized	– 1.5T GE Signa Echospeed (software N/S)	– N/S	Clinical and DBS device assessment after MRI. DBS ON/OFF.	– IPG dysfunctions during scanning – No patient adverse effects – SAR: N/S

		and internalized)				
Tronnier (1999) (54)	25	i. Medtronic ii. 3387, 3388, 3389 iii. Platinum-iridium iv. Itrel II, Itrel 3 (internalized)	– 1.5T Picker International Edge (software N/S) – 0.25T Picker International Outlook (software N/S)	– Head-transmit/head-receive – Body-transmit/body-receive	Clinical and DBS device assessment after MRI. DBS ON/OFF.	– IPG dysfunctions during scanning – No patient adverse effects – SAR: N/S
Uitti (2002) (126)	5	i. Medtronic ii. 3387, 3389 iii. Platinum-iridium iv. Itrel II (internalized)	– 1.5T GE Horizon LX (software N/S)	– N/S	Lead movement during MRI. DBS OFF.	– No significant lead movement – No patient adverse effects – SAR: N/S
Kovacs (2006) (127)	34	i. Medtronic ii. N/S iii. N/S iv. Soletra, Kinetra (internalized)	– 1.0T Siemens Magnetom Harmony. Syngo MR 2004A 4VA25A software	– Head-transmit/head-receive	Clinical assessment after MRI. DBS OFF.	– No patient adverse effects (SAR up to 0.12 W/kg)
Philips (2006) (64)	5	i. Medtronic ii. 3387, 3389 iii. N/S iv. Soletra	– 3.0T Siemens Allegra, Numaris Syngo v. VA21C software	– N/S	Clinical assessment after MRI. DBS ON/OFF.	– No patient adverse effects
Larson (2008) (22)	405	i. Medtronic ii. 3387 iii. N/S iv. Itrel II, Soletra, Kinetra (internalized) i. ANS ii. Quattrode iii. N/S iv. Libra (internalized)	– 1.5T Siemens Magnetom Vision (software N/S) – 1.5T Siemens Magnetom Symphony (software N/S) – 1.5T Philips Intera, Achieva release 1.5 software – 1.5T GE Horizon (software N/S)	– Body-transmit/head-receive – Head-transmit/head-receive	Clinical and DBS device assessment after MRI. DBS OFF.	– No patient adverse effects (SAR up to 3.0 W/kg) – No IPG dysfunction
Tagliati (2009) (11)	3481 (42 centers)	N/S	– 1.0T/1.5T GE/Siemens/Philips (software and model N/S)	– N/S	Clinical and DBS device assessment after MRI (DBS activity: N/S).	– No patient adverse effects – Single IPG dysfunction during scanning
Chhabra (2010) (70)	64	i. Medtronic ii. N/S iii. N/S iv. Itrel II, Soletra (internalized)	– GE Signa – Philips Achieva – Siemens Symphony (field strengths, softwares N/S)	– Body-transmit/head-receive	Clinical assessment after MRI. DBS OFF.	– No patient adverse effects (SAR up to 0.8 W/kg) – Perielectrode acute postoperative changes on MRI
Fraix (2010) (71)	570	i. Medtronic ii. 3387, 3388, 3389 iii. N/S iv. Itrel I, Itrel II, Soletra, Kinetra (internalized)	– 1.0T/1.5T Philips Gyroscan ACS ii (software N/S)	– Body-transmit/head-receive – Body-transmit/body-receive	Clinical and DBS device assessment after MRI. DBS OFF.	– No patient adverse effects (SAR up to 2.4 W/kg and spine SAR up to 4.0 W/kg) – No IPG dysfunction when magnet reed switch disabled
Nazzaro (2010) (72)	249	i. Medtronic ii. 3387, 3389 iii. 3550–05	– 1.5T Siemens Magnetom, VA 2.7 software	– Head-transmit/head-receive	Clinical assessment after MRI. DBS OFF.	– No patient adverse effects (SAR up to 3.1 W/kg) – Questionable IPG dysfunctions

		iv. Itrel II, Soletra (externalized and internalized)	– 1.5T Siemens Magnetom Vision/Vision Plus, Numaris 3 VG33G software			
Ullman (2011) (128)	9	i. N/S ii. N/S iii. N/S iv. N/S	– N/S	– N/S	Clinical, neuropathological, and DBS device assessment after MRI. DBS OFF.	– No patient adverse effects – No neuropathological adverse effects – No IPG dysfunction
Sammartino (2017) (40)	10	i. Medtronic ii. 3387 iii. N/S iv. Activa PC	– 3.0T GE Signa Excite (software N/S)	– Body-transmit/head-receive	Clinical and DBS device assessment after MRI. DBS OFF.	– No patient adverse effects (SAR up to 2.3 W/kg) – No IPG dysfunction
Hancu (2019) (16)	13	i. Medtronic ii. 3387, 3389 iii. 37086 iv. Activa PC	– 1.5T GE HDx – 3.0T GE Architect – 3.0T GE HDx (softwares N/S)	– Body-transmit/head-receive – Head-transmit/body-receive	Clinical and DBS device assessment after MRI. DBS ON.	– No patient adverse effects (SAR up to 0.3 W/kg and B_{1+rms} up to 1.32 uT) – Impedances stable
Boutet (2019) (12)	41	i. Medtronic ii. 3387 iii. 37086 iv. Activa PC	– 3.0T GE Signa HDx, HDx v. 16.0 V02 1131.a software	– Head-transmit/head-receive	Clinical and DBS device assessment after MRI. DBS ON.	– No patient adverse effects (SAR up to 0.3 W/kg and B_{1+rms} up to 1.8 uT) – Impedances stable
Boutet (2019) (73)	102	i. Medtronic ii. 3387, 3389 iii. 37086 iv. Activa PC/RC/SC	– 3.0T GE Signa, HDx v. 16.0 V02 1131.a software – 1.5T GE Signa, HDxT v. 23.0_V02_1406.a software – 3.0T GE Signa, Architect v. 27/LX/MR software	– Body-transmit/head-receive – Head-transmit/body-receive	Clinical and DBS device assessment after MRI. DBS ON.	– No patient adverse effects (SAR up to 1.09 W/kg and B_{1+rms} up to 1.40 uT) – Impedances stables

Abbreviations: B_{1+rms} = root-mean-square value of the MRI effective component of the RF magnetic [B1] field, DBS = deep brain stimulation, GE = General Electric, IPG = implantable pulse generator, kg = kilograms, MRI = magnetic resonance imaging, N/S = not specified, No. = number, SAR = specific absorption rate, W = watts.

References

121. Mohsin SA. Concentration of the Specific Absorption Rate Around Deep Brain Stimulation Electrodes During MRI. Prog Electromagn Res 2011;121:469–484.

122. Shrivastava D, Abosch A, Hanson T, et al. Effect of the extracranial deep brain stimulation lead on radiofrequency heating at 9.4 Tesla (400.2 MHz). J Magn Reson Imaging 2010;32(3):600–607.

123. Gorny KR, Presti MF, Goerss SJ, et al. Measurements of RF heating during 3.0-T MRI of a pig implanted with deep brain stimulator. Magn Reson Imaging 2013;31(5):783–788.

124. Shi L, Yang AC, Meng DW, et al. Pathological alterations and stress responses near DBS electrodes after MRI scans at 7.0T, 3.0T and 1.5T: an in vivo comparative study. PLoS One 2014;9(7):e101624.

125. Chen YC, Li JJ, Zhu GY, et al. Ultra-high magnetic resonance imaging (MRI): a potential examination for deep brain stimulation devices and the limitation study concerning MRI-related heating injury. Neurol Sci 2017;38(3):485–488.

126. Uitti RJ, Tsuboi Y, Pooley RA, et al. Magnetic resonance imaging and deep brain stimulation. Neurosurgery 2002;51(6):1423–1428; discussion 1428–1431.

127. Kovacs N, Nagy F, Kover F, et al. Implanted deep brain stimulator and 1.0-Tesla magnetic resonance imaging. J Magn Reson Imaging 2006;24(6):1409–1412.

128. Ullman M, Vedam-Mai V, Krock N, et al. A pilot study of human brain tissue post-magnetic resonance imaging: information from the National Deep Brain Stimulation Brain Tissue Network (DBS-BTN). Neuroimage 2011;54(Suppl 1):S233–S237.